Systemic Inflammation, the Peripheral Blood Transcriptome, and Primary Melanoma

JID Open

Juliette Randerson-Moor[1], John Davies[1,2], Mark Harland[1], Jérémie Nsengimana[3], Theophile Bigirumurame[3], Christopher Walker[1], Jon Laye[1], Elizabeth S. Appleton[1,4], Graham Ball[5], Graham P. Cook[1], D. Timothy Bishop[1], Robert J. Salmond[1] and Julia Newton-Bishop[1]

Peripheral blood transcriptomes from 383 patients with newly diagnosed melanoma were subjected to differential gene expression analysis. The hypotheses were that impaired systemic immunity is associated with poorer prognosis (thicker tumors and fewer tumor-infiltrating lymphocytes) and evidence of systemic inflammation (high-sensitivity CRP and fibrinogen levels). Higher fibrinogen levels were associated with thicker primary tumors. In single-gene analysis, high-sensitivity CRP levels were significantly associated with higher blood *CD274* expression (coding for PD-L1), but each was independently prognostic, with high-sensitivity CRP associated with increased mortality and higher *CD274* protective, independent of age. Pathway analysis identified downregulation of immune cell signaling pathways in the blood of people with thicker tumors and notable upregulation of signal transducer and activator of transcription 1 gene *STAT1* in people with brisk tumor-infiltrating lymphocytes. Transcriptomic data provided evidence for increased NF-kB signaling with higher inflammatory markers but with reduction in expression of HLA class II molecules and higher *CD274*, suggesting that aberrant systemic inflammation is a significant mediator of reduced immune function in melanoma. In summary, transcriptomic data revealed evidence of reduced immune function in patients with thicker tumors and fewer tumor-infiltrating lymphocytes at diagnosis. Inflammatory markers were associated with thicker primaries and independently with death from melanoma, suggesting that systemic inflammation contributes to that reduced immune function.

Keywords: Breslow, *CD274*, hsCRP, PD-L1, TILs

Journal of Investigative Dermatology (2024) **144,** 2513–2529; doi:10.1016/j.jid.2024.02.034

INTRODUCTION

The role of immunity in melanoma survival has long been evident even at presentation because detection of tumor-infiltrating lymphocytes (TILs) in primary tumors is associated with better outcomes (Elder et al, 2005). Furthermore, immunosuppressed recipients of solid organ transplants are at increased risk of melanoma and are more likely to present with higher-stage disease and to die of their melanoma (Park et al, 2020). More recently, sensitivity of melanoma to immune checkpoint blockade has been demonstrated, consistent with the presence of prior immune responses (Alexandrov et al, 2013). Expression of the immune checkpoint ligand PD-L1 by tumor cells in response to T-cell infiltration was also found to have some predictive value for response to checkpoint blockade (Gibney et al, 2016). Together, these observations suggest that melanoma is a good model to explore host responses to cancer and immunotherapy.

The first hypothesis explored in this paper was that the differential gene expression of circulating immune cells at first diagnosis is associated with evidence of immune impairment in people with melanoma with poorer prognosis. Further hypothesis is that this association might generate hypotheses relevant to putative adjuvant therapies or biomarkers. Dunn et al (2002) proposed the concept of immunoediting and consequent tumor escape, and in other cancers, local cytokine-driven inflammation has been reported to contribute to tumor cell escape from immunity (Germano et al, 2008; Tao et al, 2021). The interaction between cancer cells and local immune cells is complex such that effective adaptive immune responses may be negated by protumorigenic inflammation as we recently reported with respect to ulcerated melanoma (Davies et al, 2022; Jewell et al, 2015; Storr et al, 2012). This study was designed to explore a related hypothesis, which is that systemic chronic low-grade inflammation independent of tumor-generated inflammation may contribute to suppression of antitumor immunity and that this might be identified in circulating immune cells using transcriptomics. Chronic systemic inflammation is characterized by increased levels of IL-6 and IL-1β, which are known risk factors for cardiovascular disease; a recent phase 3 clinical trial (CANTOS; NCT01327846) in which canakinumab (a neutralizing antibody of IL-1β) was used to reduce further cardiovascular events

[1]*Division of Haematology and Immunology, Leeds Institute of Medical Research (LIMR), School of Medicine, University of Leeds, Leeds, United Kingdom;* [2]*Leeds Institute of Data Analytics, University of Leeds, Leeds, United Kingdom;* [3]*Population Health Sciences Institute, Faculty of Medical Sciences, University of Newcastle, Newcastle, United Kingdom;* [4]*Division of Radiotherapy and Imaging, The Institute of Cancer Research, London, United Kingdom; and* [5]*Medical Technology Research Centre, Anglia Ruskin University, Chelmsford, United Kingdom*

Correspondence: Julia Newton-Bishop, Leeds Institute of Medical Research (LIMR), School of Medicine, University of Leeds, Clinical Sciences Building, Leeds LS9 7TF, United Kingdom. E-mail: j.a.newton-bishop@leeds.ac.uk

Abbreviations: BMI, body mass index; FDR, false discovery rate; hsCRP, high-sensitivity CRP; STAT, signal transducer and activator of transcription; TIL, tumor-infiltrating lymphocyte; Th, T helper; TCR, T cell receptor

Received 7 August 2023; revised 18 February 2024; accepted 21 February 2024; accepted manuscript published online 5 April 2024; corrected proof published online 20 June 2024

after myocardial infarction (Aday and Ridker, 2018) showed that drug recipients (of which 70% were current and/or recent smokers) had reduced lung cancer deaths (Ridker et al, 2017). This suggests that systemic inflammation may drive cancer progression as well as cardiovascular disease and that cancer progression may be targeted by inhibition of the proinflammatory pathways.

Others have addressed the need to characterize immune responses as putative predictive biomarkers (Hogan et al, 2018) using techniques designed to identify circulating immune cell subgroups or TCR repertoires (Hogan et al, 2004). In this study, we used differential gene expression in peripheral immune cell transcriptomes as a means of understanding variation in immune cell function in association with both systemic inflammation and tumor growth. We chose this approach to investigation of immune cell function because of being both agnostic and a viable means of generating complex data in a large patient cohort in which other techniques such as single-cell RNA sequencing were not feasible in 2013 and remain very expensive today. Biomarkers must in clinical practice be robust to sample collection and processing variation, and the collection of RNA would therefore be a good candidate for biomarker development.

Our results demonstrate that there are differences in the peripheral blood transcriptome of patients with newly diagnosed melanoma associated with the presentation of thicker tumors and with fewer TILs. There were particularly marked transcriptomic differences associated with higher inflammatory markers consistent with the view that chronic low-grade systemic inflammation suppresses adaptive immunity at least in part by upregulating checkpoint molecules (PD-L1).

RESULTS

A total of 393 newly diagnosed participants were recruited between 2013 and 2016. Two withdrew, so data presented are derived from the 391 samples taken within 4 weeks of recruitment.

The characteristics of the participants, for example, age, biological sex, and American Joint Committee on Cancer stage at diagnosis, and the data they provided by questionnaire are shown in Supplementary Table S1. The mean age at recruitment was 64 years in men and 61 years in women, and the median age 65 years overall. Men were more likely to have thicker tumors at age <65 years ($P = .04$) but not at age >65 years (Fisher's $P = .6$) and to have higher-stage tumors at age <65 years (Supplementary Table S1) (Fisher's exact $P = .02$) but not at age >65 years (Fishers exact $P = .6$). Tumors were more commonly on the trunk in men and the limbs in women, consistent with findings from previous population studies (Yuan et al, 2019) (Supplementary Table S1).

Prevalence of reported lifestyle factors and comorbidities associated with age and sex

The reported lifestyle/comorbidities were consistent with the age and sex distribution of the cohort (Supplementary Table S1). Men were more likely to have smoked in the past ($P = .04$) and more heavily (median = 19.5 pack years in men vs 12 in women), but this was driven by participants aged >65 years. Men were also more likely to report having drunk alcohol in the preceding week ($P = .002$) and to report higher consumption (median = 14 units compared with 9 in women). Men had higher body mass index (BMI), although the difference between men and women after age 65 years was smaller, and they had correspondingly significantly greater waist/hip ratios. Men were more likely than women to report a history of hypertension, especially at age <65 years, or to have reported an angina/heart attack (age >65 years) and to have taken aspirin and/or statins at any stage, although there was no difference in reported usage at diagnosis of melanoma (at all ages).

Biomarkers of systemic inflammation variation by sex and comorbidities

Because of the distribution of high-sensitivity CRP (hsCRP) and fibrinogen levels, logarithmic transformation was performed. Log10 hsCRP (median = 1.39, interquartile range = 2.8) and fibrinogen levels (log10 median = 2.8, interquartile range = 0.9) were positively correlated with each other (Spearman's r = 0.50, $P < .0001$). The results of regression of log10(hsCRP) and log10(fibrinogen) with demographic and pathological features are shown in Supplementary Table S2. Both were marginally lower in men and were, as expected from the literature, higher in those with obesity and in older persons, but each measure had different associations with comorbidities. In univariate analysis, fibrinogen levels positively correlated ($P < .05$) with BMI, waist–hip ratio, hypertension, and smoking. For hsCRP, similar analysis showed associations with BMI, waist–hip ratio, <7 hours of sleep per night, current smoking, and lack of exercise. Those who had been exposed to statins had significantly reduced levels of hsCRP ($P = .003$). Notably, self-reported inactivity and obesity were much stronger predictors of higher levels of inflammatory markers than reported associated comorbidities. The measured levels were therefore subsequently used as a marker of morbidities in association studies.

Hematological and biochemical parameters associated with prognostic factors for melanoma

These data are presented in Supplementary Tables S3–5. Higher fibrinogen levels were more strongly associated with thicker tumors in a multivariable analysis than was hsCRP (estimate [standard error] =1.68; $P \leq .001$) (linear regression is shown Supplementary Table S4) and ulceration, albeit nonsignificantly (OR [95% confidence interval] = 5.88; $P = .1$) (Supplementary Table S3). Coulter counter neutrophil counts were significantly higher in association with both hsCRP and fibrinogen levels ($P < .001$ and $P < .001$, respectively). Positive associations were seen between hsCRP and Coulter counter–measured basophils ($P = .02$), monocytes ($P = .02$), and lymphocytes ($P = .04$) and with fibrinogen for lymphocytes ($P = .001$) and platelets ($P = .002$) (data not shown). Supplementary Table S5 shows the analysis of blood parameters in association with the histopathological features of the tumor shown as out of the normal range.

Participants with thicker tumors were more likely to have (in univariate analyses) lower vitamin D ($P = .05$), eosinophil counts ($P = .02$), and mean corpuscular volume ($P = .06$) (most frequently attributable to iron deficiency or chronic inflammatory disease). All these factors were independently predictive in multivariate analysis adjusted for age, sex, and

season of blood sampling ($P < .05$) (Supplementary Table S4) except for mean corpuscular volume. No factors were significant at $P < .05$ in the analysis of association with ulceration or the presence of brisk TILs, although higher eosinophils ($P = .07$) approached significance in multivariate analyses (OR = 0.37, 95% confidence interval CI = 0.12−1.08). Thus, thicker tumors were associated with higher inflammatory markers, lower vitamin D levels, and (borderline) mean corpuscular volume in age-adjusted analyses, consistent with late presentation or deleterious effect on tumor growth in individuals with poorer health manifest as higher inflammatory markers. Supplementary Table S6 shows the distribution of histological markers of poor outcome in the population studied.

Gene signal of immune cell subgroups in the blood

We used differential gene expression signatures (Poźniak et al, 2019) to infer 27 immune cell scores in the peripheral blood transcriptome and tested their association with sex and hsCRP (Table 1a. There were differences by sex: NK T cell ($P = .0001$), activated CD4+ T cell ($P = .001$), CD56^{bright} NK cell ($P = .001$), and effector memory CD8+ T cell ($P = .004$) scores were all significantly lower in women after allowing for multiple testing correction. In the CIBERSORT analysis (shown in supplementary information Excel file), a number of inferred cell types were also lower in women (resting mast cells, $P = .0002$; CD8+ T cells, $P = .003$; monocytes, $P = .007$; and resting dendritic cells, $P = .04$). It is clear that it was difficult to compare the 2 approaches given that they purport to infer different cell types but that in both analyses, there were differences by sex, and therefore, analyses were adjusted for sex. In the following analyses, the CIBERSORT comparisons are reported when the 27 immune cell score system describes inference of the same cell type.

Fibrinogen levels were positively associated with inferred activated CD4+ T-cell ($P = .001$), neutrophil ($P = .01$) (CIBERSORT $P = .08$), mast cell ($P = .03$) ($P = .03$ CIBERSORT for activated mast cells), memory B-cell ($P = .03$) (CIBERSORT $P = .3$), and T helper (Th) 17 ($P = .05$) scores and negatively associated with immature B-cell score ($P = .02$). Similar relationships were seen for hsCRP with neutrophils and activated CD4+ T cells, but the associations were weaker. Eosinophils showed positive correlation with hsCRP ($P = .03$) (CIBERSORT not significant). The 2 systems used to infer cell types therefore suggested broad agreement of increased cells typically described as innate immunity cells in the presence of raised inflammatory markers.

We then looked at the associations with tumor characteristics: thickness, ulceration, and brisk TILs (Table 2). Many immune cell subgroup scores were associated with thinner tumors, the strongest being CD56^{dim} NK cells ($P = .01$) and NK T cells ($P = .03$) but also T cell (Th1 cells, $P = .01$; pan T cells, $P = .06$) and pan cytotoxic cell ($P = .05$) scores as well as eosinophils ($P = .02$) (CIBERSORT $P = .38$) and mast cells ($P = .03$). Higher myeloid cell scores were associated with reduced brisk TILs: macrophage ($P = .02$), eosinophil ($P = .02$) (CIBERSORT $P = .7$), neutrophil ($P = .03$) (CIBERSORT $P = .18$), and dendritic cell ($P = .03$) scores as well as Th17 scores ($P = .06$). Notably, although eosinophil scores were higher in participants with higher hsCRP and were associated with lack of brisk TILs, they were associated with thinner tumors, and this was seen for both the inferred eosinophil measures using transcriptomes (Tables 1 and 2) and Coulter counter−measured cells ($P = .001$) (Supplementary Tables S3 and S4). The associations with ulceration were weak using both methods of inference.

These results indicate that differences in inferred circulating immune cell subgroups, especially activated CD4+ T cells, correlated with fibrinogen levels and that thicker tumors were associated with lower estimates of cells active in innate and acquired immunity. Reduced brisk TILs were moreover associated with higher circulating myeloid and Th17 cell scores, suggesting that chronic systemic inflammation is associated both with tumor progression and evidence of detectable perturbation in circulating immune cells even at first melanoma diagnosis, although we were unable to corroborate these findings using CIBERSORT.

Differential gene expression pathway and network analysis of the peripheral blood transcriptome data in association with inflammatory markers

In total, transcriptomes were available from peripheral blood sampling at diagnosis of 383 of the 391 patients with melanoma after excluding 2 samples dropped because of failed

Table 1. Bioinformatic Scores Predicting Immune Cell Subgroup Signals in the Peripheral Blood at Diagnosis of Primary Melanoma: Most Significantly Associated Inferred Immune Cell Scores with Sex, hsCRP, and Fibrinogen

				hsCRP			Fibrinogen		
Cell-Type Scores	Female, Mean (SE)	Male, Mean (SE)	*P*-Value	Cell-Type Scores	Estimate (SE)	*P*-Value	Cell-Type Scores	Estimate (SE)	*P*-Value
NK T cells	−0.08 (0.04)	**0.15 (0.04)**	**.0001**	Eosinophil	0.17 (0.08)	**.03**	Activated CD4	**0.04 (0.01)**	**.001**
Activated CD4 cells	−0.07 (0.04)	**0.05 (0.03)**	**.001**	NK T cells	−0.08 (0.04)	.06	Neutrophils	**0.02 (0.01)**	**.01**
CD56^{bright} NK cells	−0.04 (0.03)	**0.07 (0.02)**	**.001**	iDCs	0.16 (0.09)	.07	Immature B cells	**−0.02 (0.01)**	**.02**
Memory B cells	0.06 (0.02)	**−0.02 (0.02)**	**.004**	Activated CD4	0.09 (0.05)	.08	Mast cells	**0.04 (0.02)**	**.03**
TFH cells	0.06 (0.02)	**0 (0.02)**	**.03**	Neutrophils	0.06 (0.04)	.09	Memory B cells	**0.04 (0.02)**	**.03**
Effector memory CD8	−0.02 (0.03)	**0.06 (0.03)**	**.04**	Tregs	0.2 (0.14)	.1	Th17	**0.03 (0.02)**	**.05**

Abbreviations: hsCRP, high-sensitivity CRP; iDC, interstitial dendritic cell; SE, standard error; TFH, T follicular helper; Th17, T helper 17; Treg, regulatory T cell.

This table shows the most significantly associated inferred immune cell scores with sex, hsCRP, and fibrinogen. The cell scores reported were selected on the basis of highest level of significance for each analysis. Significance of differences between males and females was tested using a Mann−Whitney *U* test. Differences in hsCRP and fibrinogen levels were tested using linear regression, with log(hsCRP) and log(fibrinogen) as the endpoints. All analyses of hsCRP, fibrinogen, tumor thickness, ulceration, and TILs were adjusted for age and sex, and those significant at the $P < .05$ level are shown in bold faces. These bioinformatic scores are as reported by Angelova et al, 2015.

Table 2. Bioinformatic Scores Predicting Immune Cell Subgroup Signals in the Peripheral Blood at Diagnosis of Primary Melanoma: Top Associated Angelova Cell Scores with Ulceration, TILs, and log_{10}(Breslow) Thickness

log_{10}(Breslow)			Ulceration			TILs		
Cell Type	**Estimate (95% CI)**	***P*-Value**	**Cell Type**	**OR (95% CI)**	***P*-Value**	**Cell Type**	**OR (95% CI)**	***P*-Value**
$CD56^{dim}$ NK cells	**−0.126 (−0.223 to −0.028)**	**.012**	$CD56^{dim}$ NK cells	**0.48 (0.24–0.96)**	**.04**	Macrophages	**0.46 (0.24–0.86)**	**.02**
Th1	**−0.091 (−0.162 to −0.02)**	**.013**	T cells	0.65 (0.32–1.32)	.23	Eosinophil	**0.44 (0.22–0.85)**	**.02**
Eosinophil	**−0.108 (−0.199 to −0.017)**	**.02**	Th1	0.74 (0.45–1.23)	.25	Neutrophils	**0.71 (0.53–0.96)**	**.03**
NK T cells	**−0.059 (−0.111 to −0.008)**	**.025**	Effector memory CD8	0.74 (0.44–1.25)	.26	DCs	**0.46 (0.22–0.94)**	**.03**
Mast cells	**−0.127 (−0.244 to −0.009)**	**.034**	Central memory CD4	1.33 (0.7–2.55)	.39	Immature B cells	**1.56 (1.04–2.36)**	**.03**
Cytotoxic cells	−0.047 (−0.095 to 0.001)	.054	Macrophages	0.79 (0.43–1.43)	.43	γ-δ T cells	0.59 (0.34–1.01)	.06
T cells	−0.1 (−0.203 to 0.002)	.055	Activated B cells	0.83 (0.51–1.34)	.45	Th17	0.5 (0.24–1.03)	.06
Activated B cells	−0.063 (−0.132 to 0.006)	.073	Cytotoxic cells	0.88 (0.63–1.23)	.46	Memory B cells	0.49 (0.22–1.09)	.08

Abbreviations: CI, confidence interval; DC, dendritic cell; Th1, T helper 1; Th17, T helper 17; TIL, tumor-infiltrating lymphocyte.

This table shows the top associated Angelova cell scores with ulceration, TILs, and log_{10}(Breslow) thickness. Differences in ulceration were tested using a logistic regression model, differences in TILs (absent, nonbrisk, brisk) were tested using ordinal logistic regression, and association with log_{10}(Breslow) was tested using linear regression. All analyses of tumor thickness, ulceration, and TILs were adjusted for age and sex, and those significant at the $P < .05$ level are shown in bold faces. These bioinformatic scores are as reported by Angelova et al, 2015.

quality control (samples were not available from all participants); for 8 participants, multiple samples were analyzed, and only the better-performing samples were retained. The volcano plots for association between gene expression and hsCRP, tumor thickness, ulceration, and TILs are shown in Figure 1 and in Supplementary Figure S1 for fibrinogen.

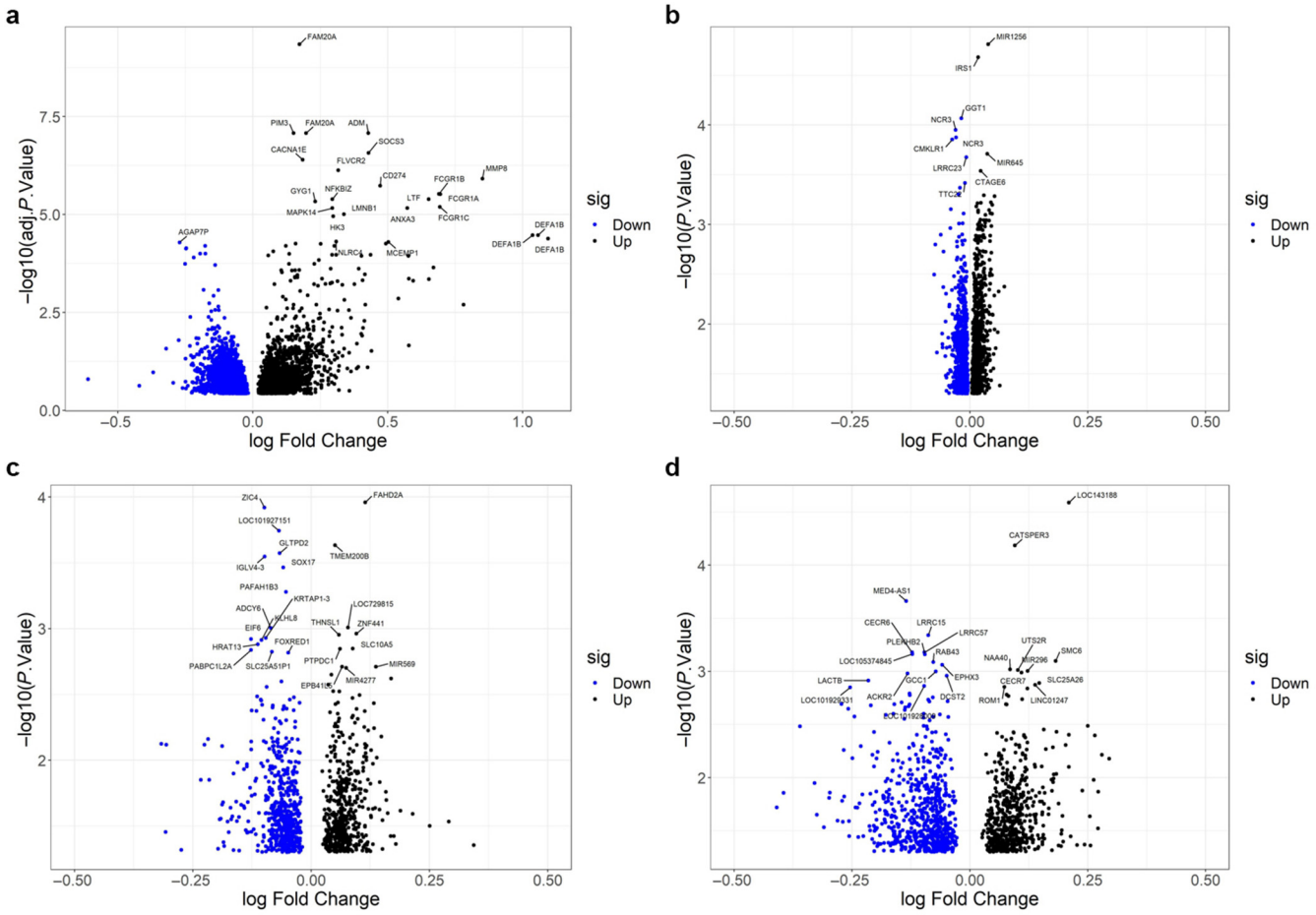

Figure 1. Volcano plots showing downregulated (blue) and upregulated (black) genes associated with key variables after correction for age and sex together with gene symbols for those genes with the smallest *P*-values. In **a**, the Y-axis reflects the adjusted *P*-value after correcting for multiple testing, whereas in **b**–**d**, *P*-values unadjusted for multiple testing. (**a**) hsCRP. (**b**) Melanoma tumor thickness (Breslow). (**c**) Ulceration. (**d**) Brisk TILs. The specific results for more detail on each plot are given in Supplementary Tables S7–S10. The volcano plot for tumor thickness analysis adjusted for sex alone (given the strong association between thickness and age) for comparison is shown in Supplementary Figure S2. hsCRP, high-sensitivity CRP; TIL, tumor-infiltrating lymphocyte.

Among all single gene studies of differential gene expression, only analysis of hsCRP showed clear, significant associations after adjusting for multiple testing with individual genes.

Genes associated with hsCRP level. Figure 1a shows that differential gene expression in association with hsCRP levels was marked (482 after adjustment for multiple testing) (Supplementary Table S7 provides the list of genes). Notably, genes known to be expressed strongly in neutrophils (coding for defensin proteins, matrix metalloproteinase 8, Fcγ receptors, and PD-L1) were all significantly overexpressed in association with higher hsCRP levels and increased fold change. Using MetaCore, analysis of genes correlated with hsCRP identified strong evidence of 2 significant networks, both identifying nodal genes in the NF-kB signaling pathway ($P = 4 \times 10^{-31}$ and 8×10^{-5}, respectively) (Figure 2) using DAVID (Database for Annotation, Visualization and Integrated Discovery) (false discovery rate [FDR] = 0.07 and Jak–signal transducer and activator of transcription [STAT] signaling FDR = 0.05). The analysis in DAVID identified an association with neutrophil extracellular trap formation (FDR = 0.02). Upregulated nodal genes included those coding for IL-10, IL-1β, TNF (TNFα), toll-like receptor 2, and IRAK4. The pathways most strongly associated are listed in Supplementary Figure S3, where Supplementary Figure S3b relates to the upregulation of IFNα/β signaling through Jak/STAT, with evidence of increased expression of *STAT1*, *STAT2*, *STAT3*, and *STAT5* and downstream genes in the presence of raised hsCRP. Notably, the network identified as significantly associated with hsCRP level was response to cytokine signaling (Figure 2c). The network analysis for fibrinogen is shown in Supplementary Figure S4d, which shows a similar association with NF-kb signaling. Supplementary Figure S3d illustrates evidence of downregulated HLA class II molecules and downregulation of Wnt-b–catenin signaling in peripheral blood cells in people with higher hsCRP, suggestive of uncontrolled IFN signaling in immune cells aberrantly associated with reduced adaptive immunity.

One of the most strongly overexpressed genes (significant after adjusting for multiple testing as well as age and sex) in association with hsCRP was *CD274* (Supplementary Table S7), which codes for PD-L1. Because IFNγ signaling regulates STAT3 and upregulates PD-L1 expression in myeloid cells, we then formally (Figure 3c) tested the association between hsCRP level and log *CD274* expression ($r = 0.33$, $P = 5.8 \times 10^{-11}$) and explored the prognostic significance of both *CD274* and hsCRP level. *CD274* expression was not associated with melanoma death in an unadjusted analysis or when adjusted for age and sex but was borderline protective when data were adjusted for hsCRP level, age, and sex ($P = .06$). In a Cox proportional hazard analysis, *CD274* and hsCRP levels were independently negatively and positively associated with death from melanoma, respectively (Figure 3c), independent of age and American Joint Committee on Cancer stage. This analysis was repeated for *CD274* and fibrinogen, and although these were positively correlated

a

	Network name	Processes	Size	Target	Pathways	*P*-value	zScore	gScore
1	NF-kB, I-kB, MyD88, IRAK4, TLR2	pattern recognition receptor signaling pathway (59.6%), positive regulation of defense response (76.6%), I-kappaB kinase/NF-kappaB signaling (51.1%), positive regulation of innate immune response (70.2%), positive regulation of response to external stimulus (78.7%)	54	25	131	3.71e-31	26.80	190.55

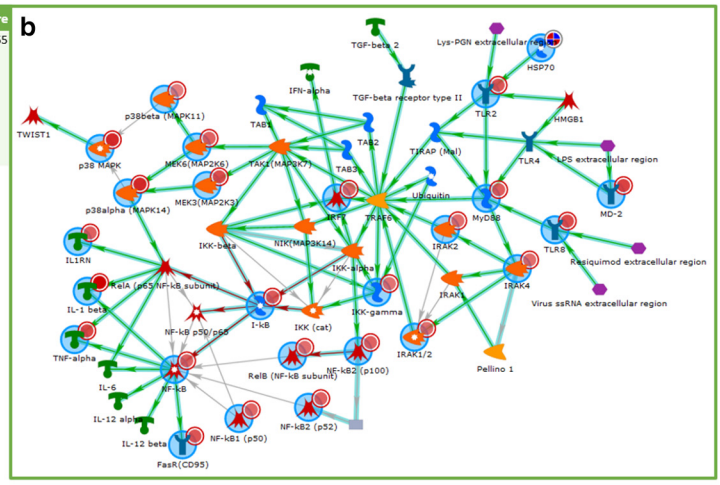

c

	Network name	Processes	Size	Target	Pathways	*P*-value	zScore	gScore
1	CREB1, JNK(MAPK8-10), JNK1(MAPK8), HSP70, CD40L(TNFSF5)	response to cytokine (90.0%), cellular response to cytokine stimulus (86.0%), response to lipopolysaccharide (70.0%), regulation of immune response (86.0%), response to molecule of bacterial origin (70.0%)	50	5	2161	8.15e-05	6.89	2708.14

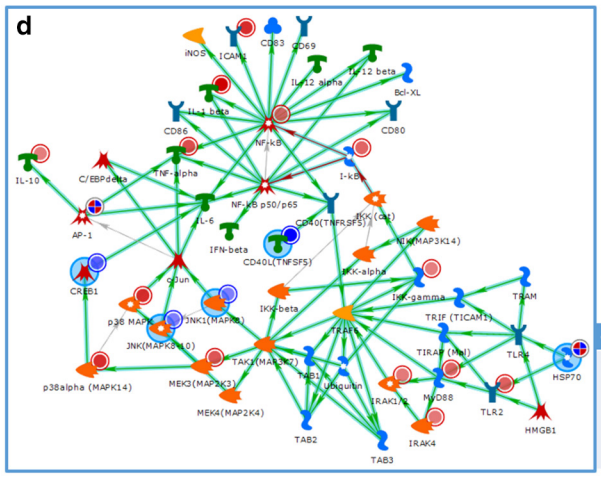

Figure 2. Illustrations generated with MetaCore pathway analysis tool (MetaCore, version 20.1, Clarivate Analytics). The map symbols description is in Supplementary Figure S2. The small red halos near the gene name illustrate the level of gene overexpression, the small blue halos illustrate the level of relative downregulation of gene expression, and the sky-blue larger halos indicate nodal genes. So, in **b**, the gene coding for IL-1β is a nodal gene that is upregulated in this analysis. (**a**) The most significantly associated process network with hsCRP in analysis of all genes differentially expressed by immune cells. (**b**) Illustration of the network in **a**. (**c**) The process network identified in analysis of genes differentially downregulated in association with hsCRP level. (**d**) Bottom left: The MetaCore figure illustrating the process network. The networks show similar upregulation of NF-kB signaling and positive regulation of immune processes. hsCRP, high-sensitivity CRP.

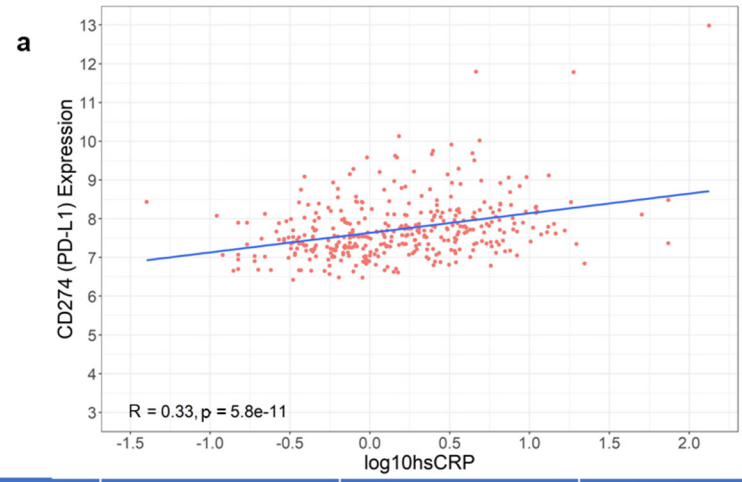

b

	unadjusted		age/sex adjusted		log_{10}hsCRP adjusted		log_{10}hsCRP/age /sex adjusted		log_{10}hsCRP/age/sex/ stage adjusted	
	HR (95% CI)	P-value	HR (95% CI)	P-value	HR (95% CI)	P-value	HR (95% CI)	P-value	HR (95% CI)	P-value
CD274 (PD-L1)	0.83 (0.60–1.15)	0.267	0.79 (0.56–1.12)	0.178	0.72 (0.51–1.02)	**0.0683**	0.70 (0.49–1.01)	**0.0585**	0.74 (0.52–1.06)	**0.0969**

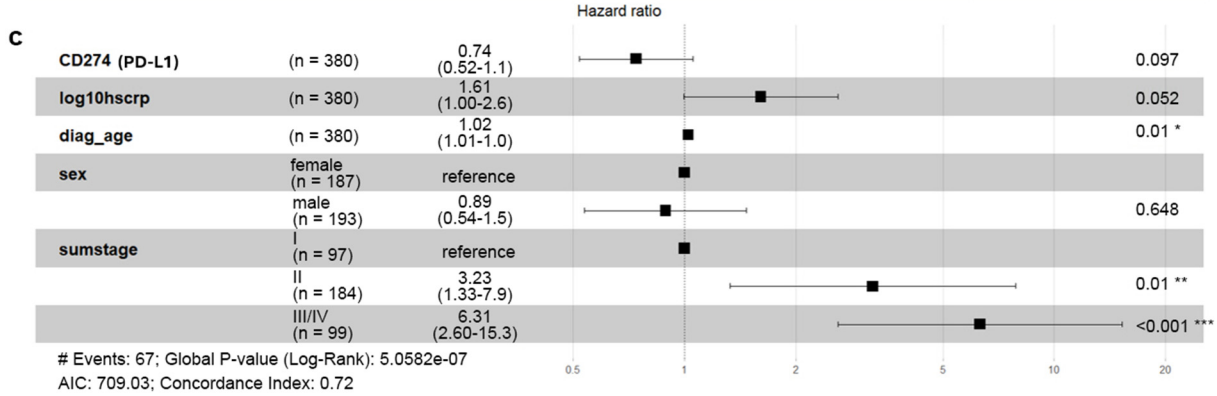

Figure 3. *CD274* expression, CRP level, and melanoma-specific survival. (**a**) The positive correlation of expressed *CD274* (which codes for PD-L1) in circulating immune cells and measured serum hsCRP at baseline in 368 patients. (**b**) A univariable analysis of immune cell expression of *CD247* and melanoma-specific survival in an unadjusted analysis and then adjusted progressively for hsCRP level, age, and biological sex. (**c**) An analysis of melanoma-specific survival in this cohort using Cox proportional hazards. Participants were recruited to the study from the dermatology service. This analysis uses stage after further investigation. The hazard ratio for death from melanoma was independently associated with *CD274* expression, with higher levels of *CD274* predicting improved survival from melanoma; hsCRP level was independently associated with increased risk of death and so, as expected, were older age at diagnosis and AJCC stage. AJCC, American Joint Committee on Cancer; CI, confidence interval; hsCRP, high-sensitivity CRP.

($r = 0.22$, $P = 2 \times 10^{-5}$), there was no significant correlation between fibrinogen and *CD274* expressions with death from melanoma in a multivariable analysis (data not shown).

Genes associated with Breslow thickness. Genes differentially expressed by circulating immune cells correlated with tumor thickness are illustrated in Figure 1b and listed in Supplementary Table S8. No single gene was significant after correction for multiple testing. Pathway enrichment analysis was carried out with genes differentially expressed at the $P <$ .05 level before correction for multiple testing in an analysis adjusted for age and sex. Because tumor thickness is known to increase with age, the analysis was repeated, adjusting for sex alone (Supplementary Figure S4), which resulted in a small change in the levels of significance but little change in the genes identified.

The pathway analysis of genes downregulated in participants with thicker tumors is shown in Figure 4. A significantly associated pathway was the role of IL-8 in melanoma (Figure 4a), and MetaCore pathway image shows evidence of increased expression of *TNF* and reduced expression of a range of genes coding for integrins such as ITGB2, which is important for extravasation of immune cells from blood into tissues (Zhang and Wang, 2012). The analysis also identified 2 networks listed in Figure 4b and illustrated in Figure 4c and d. The network most strongly associated with tumor thickness identified downregulation of signal transduction processes, particularly those involved in immune responses to microbiol molecules and IL-1 signaling in the circulating immune cells of people with thicker tumors. The nodal genes in these networks were generally negatively associated with thickness and include genes such as *NFKB*, *HSP70*, matrix metalloproteinase 9 gene *MMP9*, *EFNA1A*, and *NOS2*. Supplementary Figure S5 lists the additional most significantly downregulated genes in people with thicker tumors, such as those coding for NKG7 (*NKG7*) and RNases 2 and 3. In summary, thicker tumors were associated with downregulation of signal transduction pathways relevant to cell migration and responses to foreign

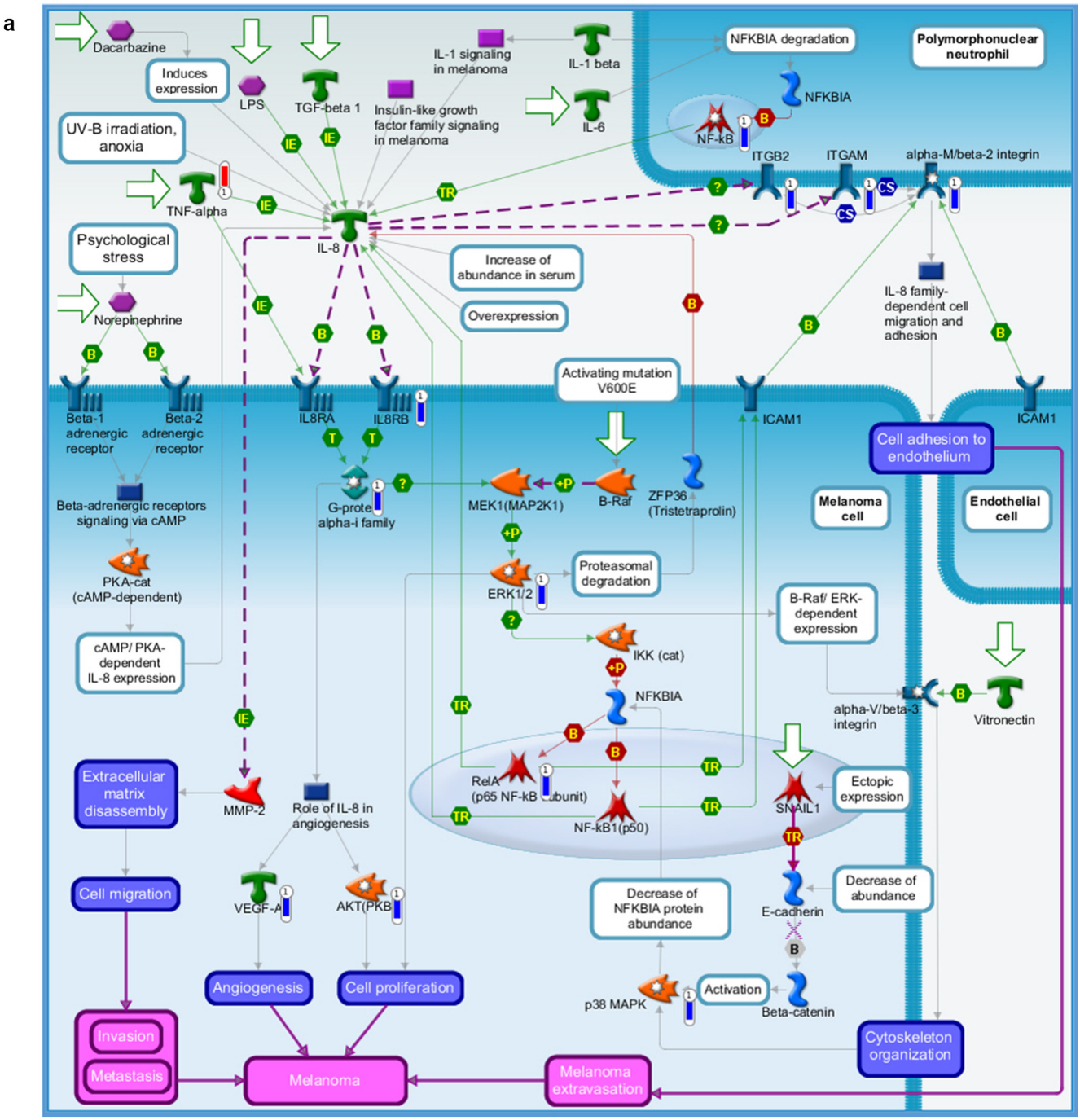

Figure 4. Pathway analysis of genes differentially expressed (downregulated) in circulating immune cells in association with tumor thickness (adjusted for age and sex) significant at $P < .05$ before correction for multiple testing. In MetaCore images, the thermometer-like symbols adjacent to the gene name indicate genes upregulated (thermometer is red) or downregulated (thermometer is blue). (**a**) Pathway significantly associated with thicker tumors, labeled IL-8 signaling in melanoma. (**b**) Two significant process networks identified as associated with thickness. (**c**) A MetaCore-generated network figure illustrating the most significantly associated network whose processes relate to downregulated nodal genes involved in signal transduction. The blue haloes in the identified 2 networks shown in **c** and **d** indicate downregulated nodal genes. (**d**) The second network in which nodal genes positively regulating immune processes were downregulated in association with thicker more advanced tumors. ERK, extracellular signal–regulated kinase; LPS, lipopolysaccharide; MEK, MAPK/ ERK, extracellular signal–regulated kinase kinase; STAT, signal transducer and activator of transcription; TLR, toll-like receptor.

antigens, suggestive of a role for the systemic immune system in control of tumor growth in early disease.

Genes associated with ulceration. The presence versus absence of reported ulceration was analyzed: none of the genes individually survived correction for multiple testing (Figure 1c). A total of 1717 transcripts differentially expressed at the $P < .05$ level before correction for multiple testing were used in a MetaCore pathway analysis (genes are listed in Supplementary Table S9). Supplementary Figure S6a

b	Network name	Processes	Size	Target	Pathways	*P*-value	zScore	gScore
1	Ephrin-A, ERK1 (MAPK3), G-protein alpha-i family, ERK1/2, TCIRG1 (Atp6i)	ephrin receptor signaling pathway (47.2%), transmembrane receptor protein tyrosine kinase signaling pathway (66.0%), enzyme linked receptor protein signaling pathway (69.8%), cell surface receptor signaling pathway (83.0%), signal transduction (100.0%)	53	7	237	4.60e-09	13.91	310.16
2	NF-kB, MyD88, I-kB, p38 MAPK, HSP70	cellular response to biotic stimulus (65.3%), response to lipopolysaccharide (71.4%), positive regulation of immune system process (87.8%), cellular response to molecule of bacterial origin (63.3%), cellular response to interleukin-1 (59.2%)	50	7	106	3.02e-09	14.35	146.85

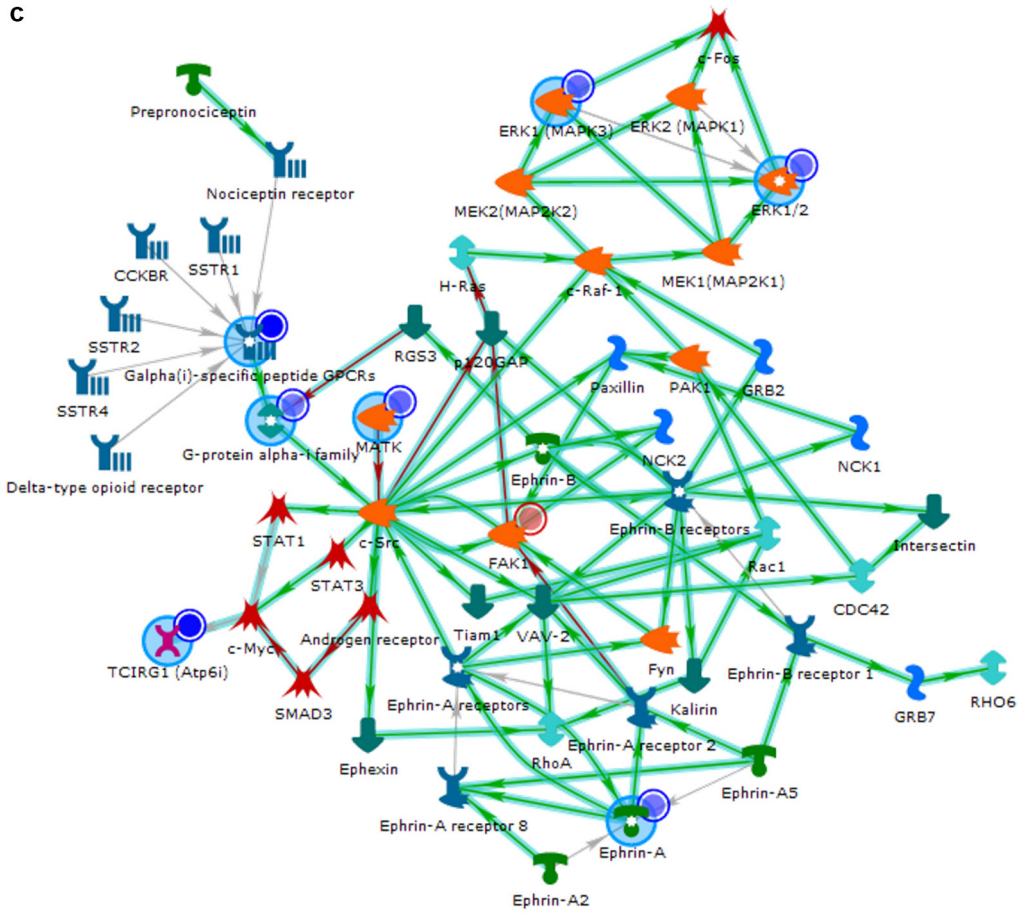

Figure 4. Continued.

and b shows the most significant pathways identified in association with ulceration, from upregulated and downregulated genes, respectively. Figure 5a and b shows the pathways associated with signaling in dendritic cells with downregulation of genes coding for HLA class II molecules. The first network identified canonical Wnt signaling as a key process ($P = 1.5 \times 10^{-4}$) (Figure 5c), with β-catenin central to the network highlighted; the second is related to innate immune responses. The third network was identified as relating to cell surface receptor signaling ($P = 9.7 \times 10^{-10}$) with downregulated nodal genes *MATK*, *MIF*, *EFNA1*, *PRL*, *CFL1*, and *KALRN*. In summary, the differential gene expression analysis identified upregulation of Wnt−β-catenin signaling and innate immune pathways in circulating immune cells of patients with ulcerated primaries, consistent with a proinflammatory status.

Genes associated with TILs. Differential gene expression associated with histologically reported brisk compared with nonbrisk or absent TILs identified 3862 genes; none individually survived correction for multiple testing (Supplementary Table S10). The pathways associated with significance at $P <$ .05 were predictably associated with immune responses. The upregulated gene pathway analysis of genes associated at $P <$ .05 (Figure 6a) identified pathways significantly related to T and B-cell receptor signaling (Figure 6b), notable upregulation of NF-kB pathway genes *HSP70* and *HSP60*, and the immune T-cell costimulatory receptor CD28 known to be reduced in immune cell senescence. A strong network was also identified ($P = 6.3 \times 10^{-5}$), in which nodal gene *STAT1* identifying cellular responses to cytokines and IL-1 and genes coding for heat shock proteins identified regulation of immune responses as the key processes associated with TILs. Upregulation of

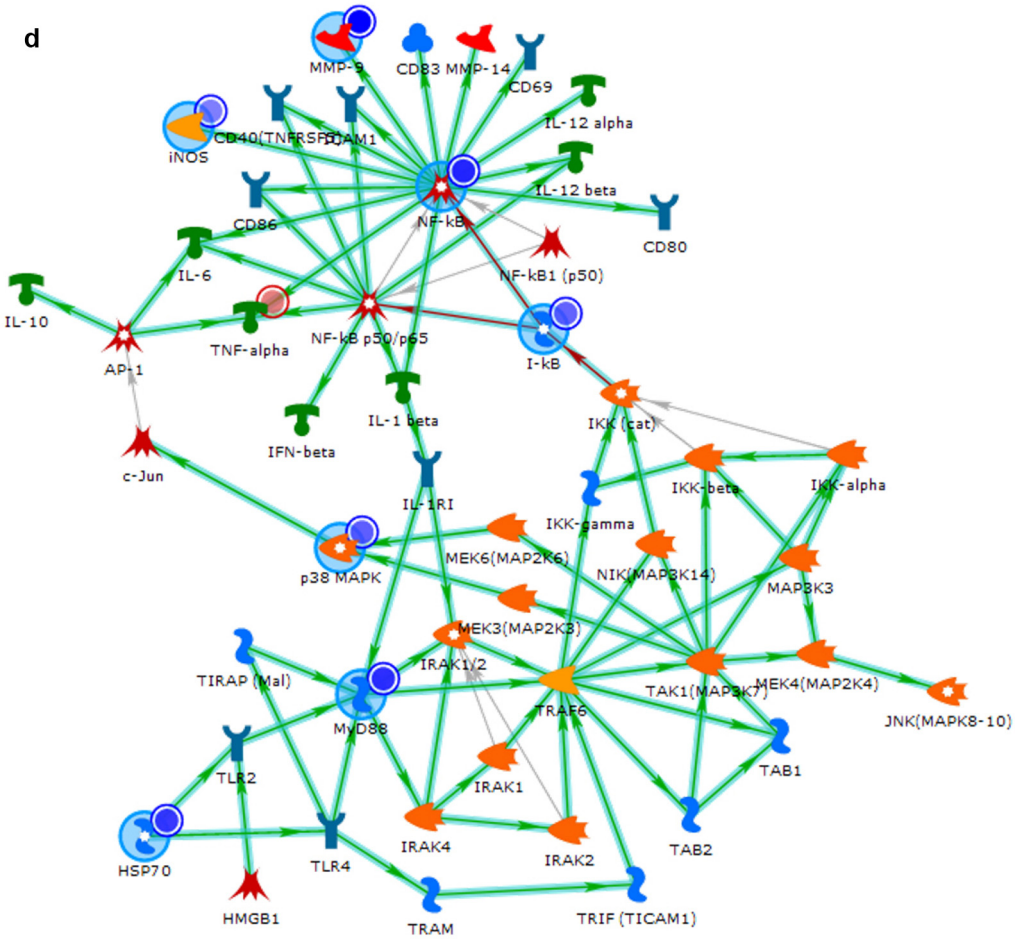

Figure 4. Continued.

nodal genes coding for STAT1, HSP60 and HSP70, and CD40 is shown in Figure 6d. These data indicate activation of circulating immune cells in people mounting a greater immune response to their primary tumors, which in individuals at first presentation to dermatology may reflect their immune health per se rather than responses to the tumor.

The transcriptome data are available on request from European Molecular Biology Laboratory. The nature of the consent obtained from participants requires that the institute requesting data must sign a data transfer agreement.

DISCUSSION

That men have a worse prognosis than women at all stages of melanoma (Joosse et al, 2013) is poorly understood. In this study, men aged <65 years more frequently presented with tumors with poorer prognosis by site (trunk) and of higher stage. If systemic inflammation plays a role in melanoma progression, then men might also be more at risk of melanoma death because of a higher prevalence of risk factors for systemic inflammation. Indeed, a history of smoking, higher BMI, waist/hip ratio, and hypertension (Naik et al, 2019) were more common in men, especially at age <65 years. Lifestyle may therefore contribute to the poorer survival in men with melanoma. Inflammatory markers were however marginally higher in women, which has been reported previously across different ethnicities even when analyses were adjusted for confounding variables (Lakoski et al, 2006). The complex relationship between obesity, sex, immune function, and response to immunotherapies is illustrated by the obesity paradox: worse outcomes for patients with obesity with cancer but better responses to immunotherapy (Naik et al, 2019). Using peripheral blood transcriptomics to better understand the role of systemic inflammation on immune responses to melanoma was the primary aim of this study and hypothesis generation with respect to potential adjuvant suppression of IL-1β signaling in at-risk patients.

Is there significant evidence of immune insufficiency in association with higher inflammatory markers?

We report higher levels of inflammatory markers in those with obesity and who reported lack of exercise. Both hsCRP and fibrinogen are acute-phase proteins synthesized in the liver, but the coagulation factor fibrinogen plays a role in chronic inflammation at least in part by binding to macrophages and activating the release of cytokines (Göbel et al, 2018). This function is consistent with our findings of a stronger positive association between scores for activated CD4+ T, neutrophil, mast, memory B, and Th17 cells and higher fibrinogen levels, although these findings reflect inference and are therefore hypothesis generating. It is of note that lower hsCRP levels were seen in participants on statins,

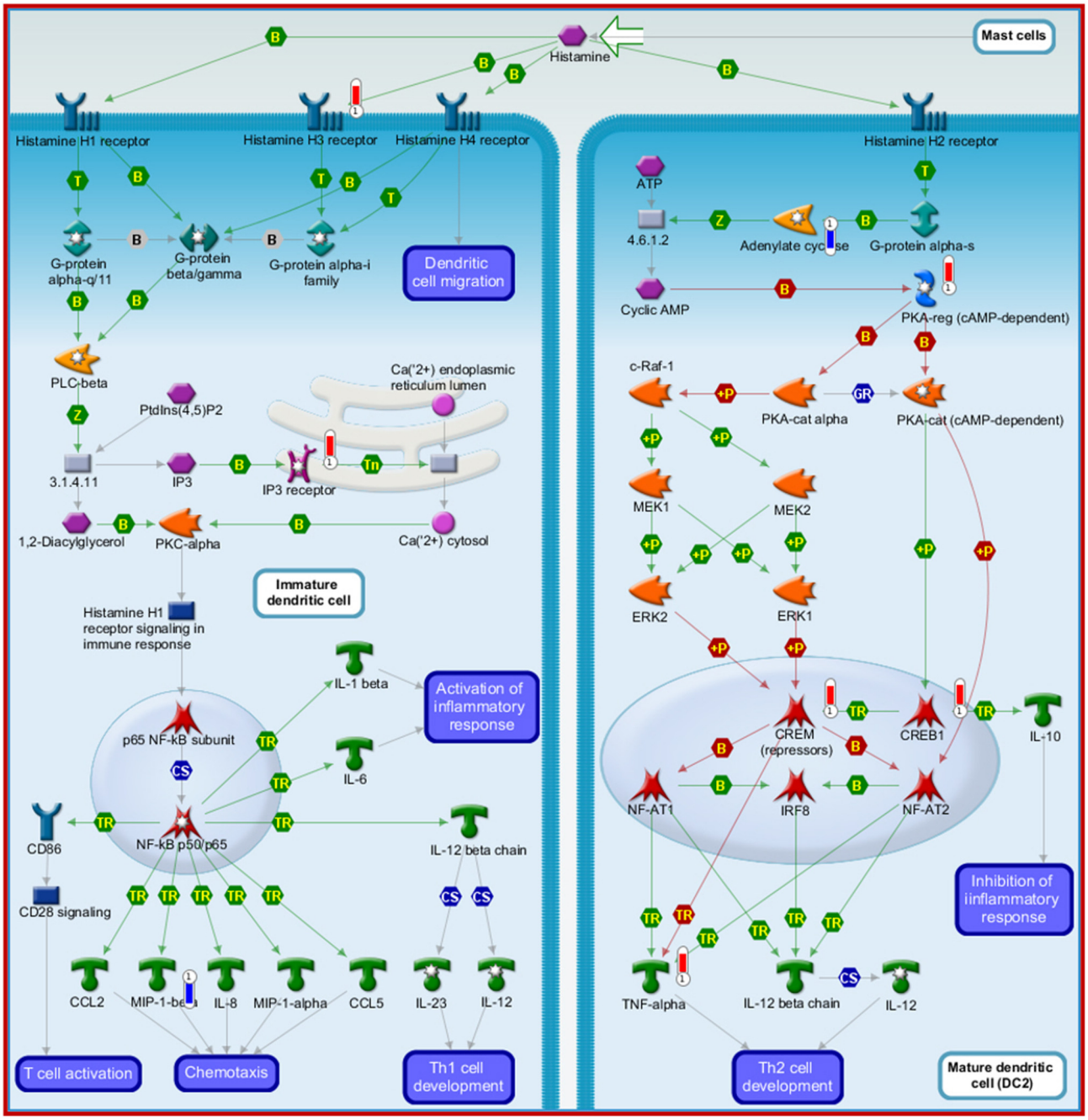

Figure 5. MetaCore pathway and network analysis of genes differentially expressed (upregulated) in circulating immune cells in association with microscopic ulceration of the primary tumor. (**a**) MetaCore image of a pathway associated with ulceration illustrating activation processes in circulating immune cells associated with dendritic cell function. In MetaCore images, the thermometer-like symbols adjacent to the gene name indicate genes upregulated (thermometer is red) or downregulated (thermometer is blue). (**b**) The 2 networks derived from the differential expression (upregulation) of immune cells in association with ulceration. (**c**) The first network listed with processes listed related to Wnt signaling. (**d**) The second network whose processes relate to activation of innate immunity. ATP, adenosine triphosphate; EGF, epidermal GF; ERK, extracellular signal–regulated kinase; MEK, MAPK/ ERK, extracellular signal–regulated kinase kinase.

suggesting a possible adjuvant function for these widely available drugs in recently diagnosed melanoma patients.

We saw fewer TILs in participants with a higher neutrophil/lymphocyte ratio and higher inferred scores for circulating macrophages, eosinophils, neutrophils, and dendritic cells, providing some observational support for a relationship between systemic inflammation, associated increase in the myeloid compartment, and impaired immune responses to melanoma. Our hypothesis was that systemic inflammation is associated with reduced antitumor responses, and in vitro data suggesting a direct inhibitory effect of hsCRP on immune cell function in vitro in melanoma were recently reported by the Weber laboratory (Yoshida et al, 2020). The peripheral blood transcriptome analysis of differential gene expression in association with hsCRP identified 2 gene networks associated with upregulation of proinflammatory NF-kb signaling

b	Network name	Processes	Size	Target	Pathways	p-Value	zScore	gScore
1	WNT, EGF, WNT7A, Beta-catenin, TCF7L2 (TCF4)	canonical Wnt signaling pathway (54.0%), cell surface receptor signaling pathway involved in cell-cell signaling (62.0%), cell-cell signaling by wnt (58.0%), Wnt signaling pathway (58.0%), regulation of cell population proliferation (86.0%)	53	3	663	1.48e-04	9.15	837.90
2	TNF-alpha, XIAP, LOC389765, NBPF10, NBPF15	I-kappaB kinase/NF-kappaB signaling (53.8%), innate immune response-activating signal transduction (53.8%), positive regulation of defense response (64.1%), activation of innate immune response (53.8%), regulation of defense response (71.8%)	48	12	356	1.18e-22	39.55	484.55

c

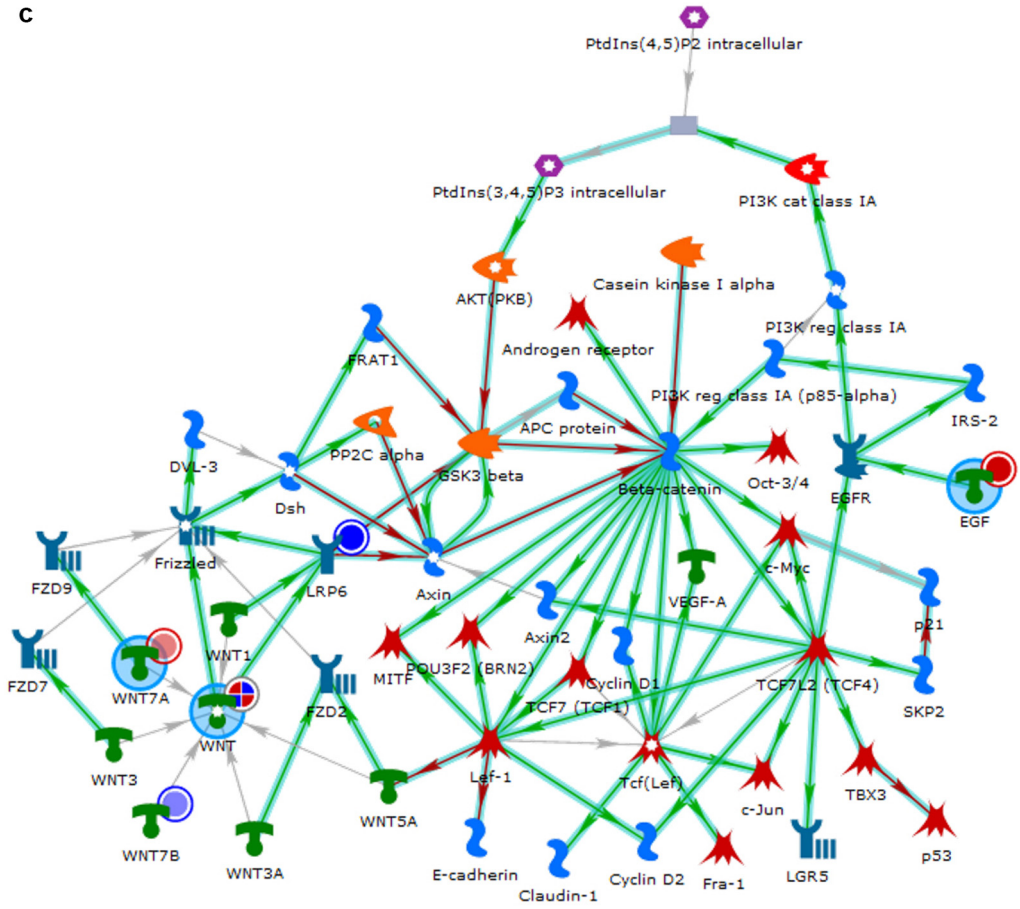

Figure 5. Continued.

in immune cells. Upregulated nodal genes were *IL1B*, *IL10*, *TNF*, and *NFKB*, and the pathway analysis (Supplementary Figure S3) identified IFN-γ signaling as upregulated with increased *STAT1*, *STAT2*, and *STAT3*. Conversely, the pathway analysis also indicated reduced expression of HLA class II genes, which would normally be increased as a result of NF-kB signaling in adaptive immunity. We argue that the IFN signaling is aberrant given the higher levels of *STAT3*, concurrent increased expression of *IL1B*, and reduced expression of HLA class II genes. Downregulation of HLA molecules was previously reported in circulating immune cells to predict poorer response to immunotherapy (Krieg et al, 2018; Yi et al, 2017). That we report evidence of reduced expression of HLA class II genes in the peripheral blood patients with fewer TILs at first presentation to the dermatologist argues that clinically significant peripheral immune suppression may be detectable in patients long before widespread metastasis is detected. Jak/STAT signaling in response to cytokines plays a critical role in activation of immune responses, but aberrant activation may drive inflammatory diseases (Shen-Orr et al, 2016; Yan et al, 2018). IFN-γ signaling also increases PD-L1 expression in myeloid cells, and in this study, we report a strong positive association of *CD274* expression in circulating immune cells with hsCRP levels. PD-L1 expression in immune cells is reported to be greatest in macrophages (Liu et al, 2020) and moreover to predict better outcomes from immunotherapy, and we were able to confirm an association of increased *CD274* expression in immune cells associated with a better outcome in the dataset, although only in a multivariable analysis, with hsCRP, age, and sex. These data imply that patients with both high *CD274* expression and higher levels of hsCRP are less likely to survive and therefore that *PDL1* expression here may reflect a feedback response to IFN-γ signaling in aberrant

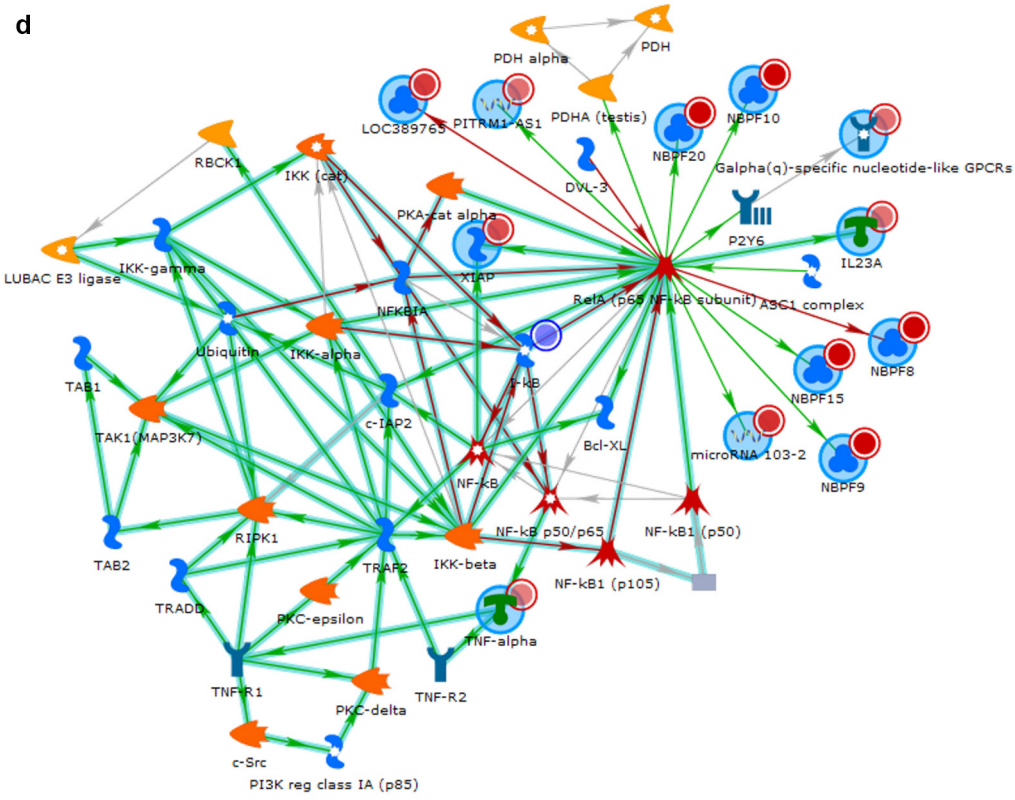

Figure 5. Continued.

systemic inflammation suppressing effective antitumor responses. High CD274 and low hsCRP are associated with better survival, indicating more effective antitumor responses.

Inflammatory markers, inferred circulating white cell subgroups, and progression of primary melanoma

If systemic inflammation is associated with reduced antitumor immunity, we postulated that tumor growth prior to resection would result in thicker, more frequently ulcerated primaries. We report evidence for that because fibrinogen level was independently associated with thicker tumors, although not significantly with ulceration or TILs.

Higher serum vitamin D levels were associated with thinner tumors, and vitamin D is reported to be negatively correlated with systemic inflammation (Amer and Qayyum, 2012; Liu et al, 2018), but we have also previously reported that vitamin D/vitamin D receptor signaling inhibits tumor growth by suppressing β-catenin signaling in a different dataset (Muralidhar et al, 2019).

In this study, we report that the inferred cell scores active in both innate and adaptive immunity were associated with thinner tumors, which lends support to the hypothesis that individual variation in immune health is related to control of tumor growth.

The analysis of differential gene expression pathway analysis of immune cells in association with thicker tumors showed downregulation of signal transduction pathways and pathways related to innate immunity. The network analysis suggests reduced receptor signaling pathways, especially relating to ephrin-mediated trafficking of immune cells (Darling and Lamb, 2019), and reduced innate immune responses are associated with thicker tumors, suggestive of a role for systemic immune responses in the progression of primary tumors.

The presence of microscopic ulceration in primary tumors is an independent predictor of melanoma death. The pathway analysis for ulceration was similar to that for thickness because ephrin receptor signaling was the network downregulated in ulcerated tumors and evidence for reduced expression of HLA class II molecules. Ephrin receptors and ligands are recognized to play a significant role in immune cell function, including cell trafficking (Darling and Lamb, 2019), which is crucial to immune responses to cancers. However, there was a notable association between upregulated canonical Wnt signaling in immune cells and tumor ulceration identified in the network analysis, with increased expression of nodal genes coding for WNT7A (which is primarily released by CD3 lymphocytes in the blood [Ochoa-Hernández et al, 2012]) and epidermal GF and reduced expression of *LRP6*. Ulceration and thickness are strongly associated, so that these similarities are not surprising but speak to similarly associated inflammatory processes in circulating immune cells.

It was hypothesized that pathway analysis of differentially expressed genes would inform an understanding of immune responses to the tumor (Krijgsman et al, 2019), and the pathway analysis provided evidence that upregulation of genes mediating T and B-cell receptor signaling predicted more TILs. The network identified upregulated nodal genes *STAT1*, *HSP60*, *CD40*, *HSP70*, and *CD83*, which are functionally attributed to cellular responses to cytokines and

a	Maps	Total	*P*-value	FDR	In Data	Network Objects from Active Data
1	Immune response: TCR alpha/beta signaling pathway	97	3.112E-08	4.046E-05	20	Akt(PKB), STIM1, MALT1, Calcineurin A (catalytic), NF-AT2(NFATC1), PKC-theta, E2N(UBC13), MHC class II, STK39, TRAF3, Fyn, CalDAG-GEFII, PAG, Calmodulin, CD28, B-Raf, CaMK IV, IP3 receptor, CARD11, FYB1
2	CHDI: Correlations from Replication data - Causal network (positive correlations)	79	1.755E-07	1.141E-04	17	Akt(PKB), Calcineurin A (catalytic), VIL2 (ezrin), PKC-theta, CD44, CD83, MHC class II, MEKK4(MAP3K4), HSP70, PSMC2, Calmodulin, CD40(TNFRSF5), ROCK, CD28, CaMK IV, IP3 receptor, IP3R1
3	Immune response: B cell antigen receptor (BCR) pathway	110	2.777E-07	1.204E-04	20	Akt(PKB), STIM1, MALT1, Calcineurin A (catalytic), ETS1, NF-AT2(NFATC1), VAV-2, p70 S6 kinase1, MEKK4(MAP3K4), CalDAG-GEFII, Cyclin D2, Calmodulin, MEKK1(MAP3K1), SOS1, B-Raf, BLNK, c-Rel (NF-kB subunit), CDK6, IP3 receptor, CARD11
4	Microsatellite instability in gastric cancer	22	3.963E-07	1.288E-04	9	MutSalpha complex, MSH6, DNA polymerase eta, MutSbeta complex, MSH3, MutLbeta complex, MLH1, PMS1, MSH2
5	DNA damage: Role of Brca1 and Brca2 in DNA repair	30	8.361E-07	2.174E-04	10	MSH6, DDB2, MRE11, ATR, Rad50, p53BP1, MSH3, ATM, MLH1, MSH2

b

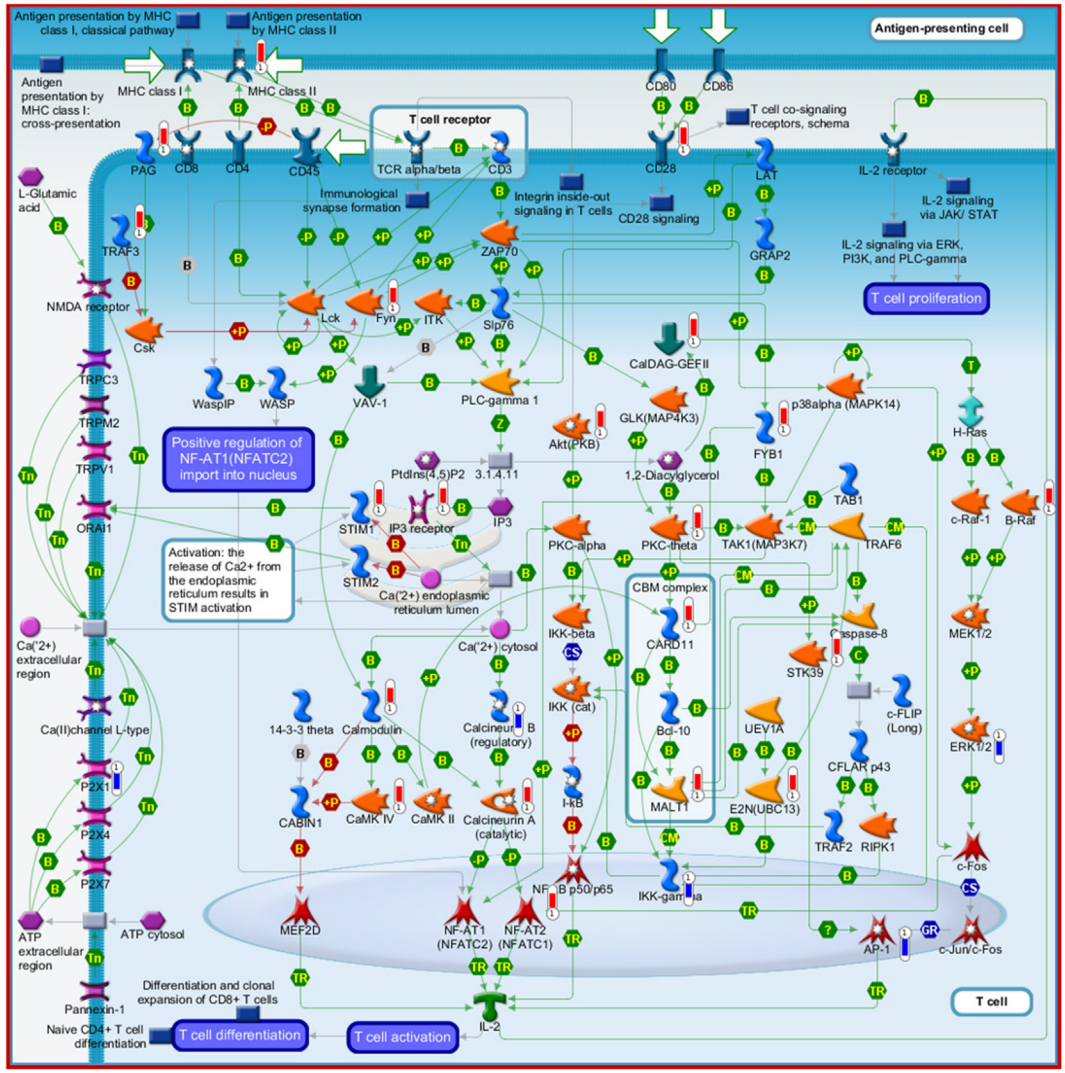

Figure 6. MetaCore output–generated pathway and network analysis of genes differentially expressed (upregulated) in circulating immune cells in association with brisk versus nonbrisk or absent TILs. (**a**) Pathways identified as associated with brisk TILs in primary melanomas. (**b**) The MetaCore image illustrating the most strongly associated pathway labeled immune response TCRα/β signaling pathway. The red thermometers illustrate upregulation of many genes in this pathway. (**c**) The network identified in association with brisk TILs labeled cellular response to cytokine stimulus. (**d**) This network illustrated with nodal genes upregulated: *CD83*, *CD40*, *STAT1*, *HSP60*, and *HSP70*. Akt, protein kinase B; AP-1, activating protein 1; MEK, MAPK/ ERK, extracellular signal–regulated kinase kinase; STAT1, signal transducer and activator of transcription 1; TIL, tumor-infiltrating lymphocyte.

C	Network name	Processes	Size	Target	Pathways	*P*-value	zScore	gScore
1	STAT1, HSP60, CD40(TNFRSF5), HSP70, CD83	cellular response to cytokine stimulus (86.0%), response to cytokine (88.0%), cytokine-mediated signaling pathway (76.0%), regulation of immune response (86.0%), cellular response to interleukin-1 (58.0%)	50	5	119	6.25e-05	7.13	155.88

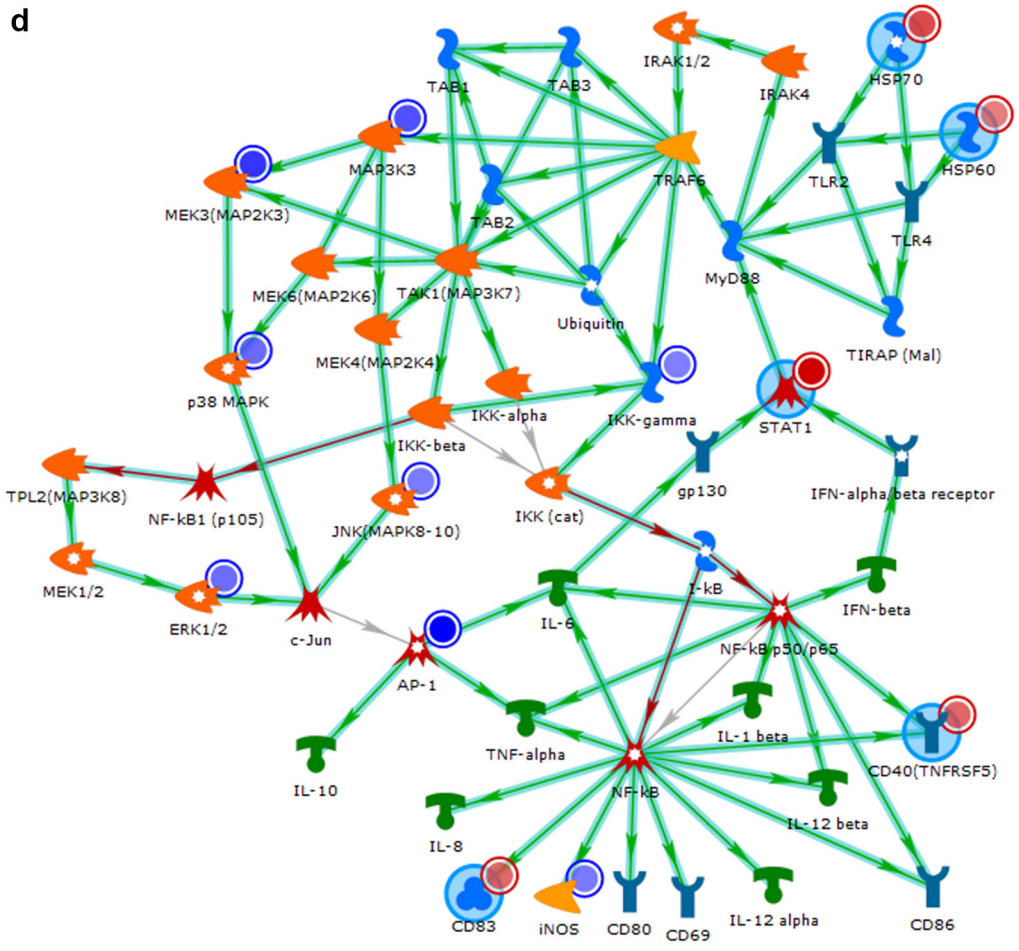

Figure 6. Continued.

reduced activated protein 1 signaling and as regulators of immune checkpoint (Atsaves et al, 2019). CD40 and CD83 are important activation markers for antigen-presenting cells, and in this context, the analysis suggests that brisk TILs are associated with increased T-cell priming. Furthermore, the observations of an association between higher eosinophil counts and thinner tumors less likely to be ulcerated are consistent with the recent report of a critical role for eosinophils and type 2 innate lymphoid cells in antimelanoma responses (Jacquelot and Belz, 2021; Jacquelot et al, 2021).

In summary, we report evidence of reduced immune function in patients with thicker tumors and fewer TILs, at diagnosis. Although it is not possible to exclude the possibility that these differences were induced by the tumor, it seems likely that these were at least in part differences in the host, which contributed to tumor progression. Inflammation, which is controlled and directed toward tumors, is crucial for survival from melanoma, but uncontrolled, aberrant inflammation such as the one that is associated with chronic diseases is harmful in the population overall. In this study, we report evidence that such aberrant inflammation (defined by higher inflammatory markers) is also important in host versus melanoma responses because higher inflammatory markers were associated with thicker primaries, higher expression of *CD274*, and death from melanoma. Markers were also associated with higher circulating myeloid cells, which were in turn associated with fewer TILs.

Importance

This study describes the immune health of patients with melanoma at first presentation to dermatologists and the role of systemic inflammation in limiting antitumor responses using the analysis of circulating immune cell transcriptomes. These observations raise the possibility of identifying blood-derived biomarkers of prognostic and predictive significance and of reducing relapse rate by modifying systemic inflammation at first diagnosis.

MATERIALS AND METHODS

Study overview

The vitamin D and immunity study is a population-ascertained primary melanoma cohort of stage IB and higher (Davies et al, 2022) at recruitment, which took place at the first visit to the Leeds

Melanoma Multidisciplinary Clinic. Participants completed a comorbidities and lifestyle questionnaire (particularly relevant to the metabolic syndrome and cardiovascular disease) at recruitment using questions previously trialed in the Leeds Melanoma Cohort (Hardie et al, 2020). BMI was calculated. Clinicopathological details of the melanoma were extracted from clinical records supplemented using national death and cancer registration records. Blood samples were taken at presentation and 4 weeks later at admission for wide local excision and sentinel node biopsy. The study was approved by the national ethics committee (REC 13-YH-0237) and was carried out according to Helsinki Treaty. All participants gave written, informed consent.

Clinicopathological data

Histopathological parameters were extracted from reports generated by the Leeds Melanoma Multidisciplinary Clinic according to protocol. TILs were categorized as described originally by Clark's group (Clark et al, 1989) as either brisk, nonbrisk, or absent. The methodology for assays of inflammatory markers, vitamin D levels, and hematological measures is provided in Supplementary Materials and Methods.

Generation of peripheral blood transcriptome data

Peripheral blood RNA was collected using the LeukoLOCK Total RNA Isolation System (Ambion, Thermo Fisher Scientific) to isolate circulating immune cells. Gene expression data were generated from RNA at either of the baseline time points (0 or 4 weeks) at whichever the hsCRP was lowest to reflect resting-state inflammation rather than that associated with concurrent infections. Whole-genome expression data were generated from RNA (200 ng) using the GeneChip Human Transcriptome Array 2.0 (Applied Biosystems, Thermo Fisher Scientific) and GeneChip WT PLUS Reagent Kit according to the instructions of a service provider (Hologic). The arrays were processed in 5 batches, followed by data cleaning and quality control of the transcriptomic data using standard procedures (Supplementary Materials and Methods).

Statistical and bioinformatic analyses

Within each biological sex and between the sexes, the distribution of clinicopathological factors between participants above and below the median age of diagnosis were assessed using chi-square tests or Fisher exact tests as appropriate.

To test the association of measured biochemical or hematological factors with inflammatory markers (log10 levels of hsCRP or fibrinogen), log(Breslow) tumor thickness, ulceration status, and the presence of recorded TILs, multivariable linear regression models adjusting for age and sex were fitted. The differences between participants were tested both as a continuous variable and for levels elevated above the normal range compared with those within the normal range (the latter as possibly being more meaningful to clinicians). Blood results for liver enzymes (alanine transaminase, aspartate transaminase, and lactate dehydrogenase); fibrinogen; hsCRP; 2 red cell markers (mean corpuscular volume and mean corpuscular hemoglobin); and Coulter counter—measured monocyte, eosinophil, neutrophil, total white cell, and platelet counts were assessed. Multivariable models were constructed separately for each endpoint containing all variables that had a significance of $P < .1$ in univariable analyses. All analyses were adjusted for age and sex using Stata 14.2 (StataCorp). Except as noted in the text, significance levels are reported unadjusted for multiple testing.

Differential gene expression was analyzed in association with inflammatory markers, tumor thickness, ulceration, and histologically reported brisk versus absent/nonbrisk TILs. In our previous work designed to interrogate the immune cell infiltration in melanoma primaries (Poźniak et al, 2019), a bioinformatic approach to inferring the presence of immune cell subsets was developed on the basis of the work of Angelova et al (2015). The Angelova immunome system was derived from transcriptomes of FACS-sorted circulating immune cells (Angelova et al, 2015). We applied the immunome deconvolution in this study to infer scores of 27 immune cell subtypes in peripheral blood using whole-genome transcriptomes. We attempted to corroborate findings by comparison with a second deconvolution tool (CIBERSORT, https://cibersortx.stanford.edu), although comparison was limited because of small numbers of cell subtypes inferred by both systems, as has been reported previously (Newman et al, 2017).

Pathway enrichment analyses of identified differentially expressed genes were performed using MetaCore, version 20.1 (Clarivate Analytics, Clarivate) (Supplementary Materials and Methods provides the details). For each variable dataset, 3 enrichment analyses were performed: (i) on the basis of all differentially expressed genes, (ii) on the basis of upregulated genes, and (iii) on the basis of downregulated genes. In this study, our interpretations have focused on the outputs of the pathway and network analyses. Where the analysis identified strong evidence of networks (gscore > 100), these are shown preferentially in the figures, over individual pathways. Where no network was identified or a pathway was illustrative of a particular immune cell function, then these were shown either in the main text or supplementary data. The DAVID Functional Annotation Bioinformatics Microarray Analysis system was used to test agreement with the results in MetaCore for hsCRP.

Ethics Statement

This study was approved by the United Kingdom national ethics review system Integrated Research Application System (number 129487). All participants gave their written, informed consent.

DATA AVAILABILITY STATEMENT

The transcriptome data are available on request from European Molecular Biology Laboratory. The contact person is JN of the University of Newcastle. Contact email address is jeremie.nsengimana@newcastle.ac.uk. The nature of the consent obtained from participants requires that the institute requesting data must sign a data transfer agreement.

ORCIDs

Juliette Randerson-Moor: http://orcid.org/0000-0003-0303-0072
John Davies: http://orcid.org/0009-0002-4272-2477
Mark Harland: http://orcid.org/0000-0002-0077-9742
Jérémie Nsengimana: http://orcid.org/0000-0002-3603-4208
Theophile Bigirumurame: http://orcid.org/0000-0003-2387-4918
Christopher Walker: http://orcid.org/0009-0006-9699-3714
Jon Laye: http://orcid.org/0009-0001-5036-7973
Elizabeth S. Appleton: http://orcid.org/0000-0002-8794-3428
Graham Ball: http://orcid.org/0000-0001-5828-7129
Graham P. Cook: http://orcid.org/0000-0003-0223-3652
D. Timothy Bishop: http://orcid.org/0000-0002-8752-8785
Robert J. Salmond: http://orcid.org/0000-0002-1807-1056
Julia Newton-Bishop: http://orcid.org/0000-0001-9147-6802

CONFLICT OF INTEREST

The authors state no conflict of interest.

ACKNOWLEDGMENTS

The source of the data was the vitamin D and immunity study, primarily supported by the Medical Research Council Project grant MR/M019012/1. Members of the research group were additionally funded by Cancer Research UK C588/A19167, C8216/A6129, and C588/A10721 and National Institutes of Health CA83115. Our thanks are to those patients who gave their time and their very blood. The order of authors was as follows. The principal investigator of the Melanoma Research Group is JN-B and is listed last, with independent RS contributing essential interpretation listed as next to last. Other senior authors GB, GPC, and DTB and the less senior authors are listed according to the relative contribution made.

AUTHOR CONTRIBUTIONS

Conceptualization: DTB, GPC, JN-B; Data Curation: JR-M, JD, MH, CW, TB, JL, DTB, RJS, JN-B; Formal Analysis: JD; Funding Acquisition: DTB, JN-B; Investigation: JR-M, JD, MH, JN, GB, DTB, GPC, RJS, JN-B; Methodology: JR-M; Visualization: JR-M; Resources: JR-M, JL, DTB, JN-B; Validation: JD; Writing – Original Draft Preparation: JN-B; Writing - Review and Editing: JR-M, JD, MH, CW, LA, JN, JL, DTB, GPC, RS, JN-B

SUPPLEMENTARY MATERIAL

Supplementary material is linked to the online version of the paper at www.jidonline.org, and at https://doi.org/10.1016/j.jid.2024.02.034.

REFERENCES

Aday AW, Ridker PM. Antiinflammatory therapy in clinical care: the CANTOS trial and beyond. Front Cardiovasc Med 2018;5:62.

Alexandrov LB, Nik-Zainal S, Wedge DC, Aparicio SA, Behjati S, Biankin AV, et al. Signatures of mutational processes in human cancer. Nature 2013;500:415–21.

Amer M, Qayyum R. Relation between serum 25-hydroxyvitamin d and C-reactive protein in asymptomatic adults (from the continuous national health and nutrition examination survey 2001 to 2006). Am J Cardiol 2012;109:226–30.

Angelova M, Charoentong P, Hackl H, Fischer ML, Snajder R, Krogsdam AM, et al. Characterization of the immunophenotypes and antigenomes of colorectal cancers reveals distinct tumor escape mechanisms and novel targets for immunotherapy. Genome Biol 2015;16:64.

Atsaves V, Leventaki V, Rassidakis GZ, Claret FX. AP-1 transcription factors as regulators of immune responses in cancer. Cancers (Basel) 2019;11:1037.

Clark WH Jr, Elder DE, Guerry D, Braitman LE, Trock BJ, Schultz D, et al. Model predicting survival in stage I melanoma based on tumor progression. J Natl Cancer Inst 1989;81:1893–904.

Darling TK, Lamb TJ. Emerging roles for Eph receptors and ephrin ligands in immunity. Front Immunol 2019;10:1473.

Davies J, Muralidhar S, Randerson-Moor J, Harland M, O'Shea S, Diaz J, et al. Ulcerated melanoma: systems biology evidence of inflammatory imbalance towards pro-tumourigenicity. Pigment Cell Melanoma Res 2022;35:252–67.

Dunn GP, Bruce AT, Ikeda H, Old LJ, Schreiber RD. Cancer immunoediting: from immunosurveillance to tumor escape. Nat Immunol 2002;3:991–8.

Elder DE, Gimotty PA, Guerry D. Cutaneous melanoma: estimating survival and recurrence risk based on histopathologic features. Dermatol Ther 2005;18:369–85.

Germano G, Allavena P, Mantovani A. Cytokines as a key component of cancer-related inflammation. Cytokine 2008;43:374–9.

Gibney GT, Weiner LM, Atkins MB. Predictive biomarkers for checkpoint inhibitor-based immunotherapy. Lancet Oncol 2016;17:e542–51.

Göbel K, Eichler S, Wiendl H, Chavakis T, Kleinschnitz C, Meuth SG. The coagulation factors fibrinogen, thrombin, and factor XII in inflammatory disorders-a systematic review. Front Immunol 2018;9:1731.

Hardie CM, Elliott F, Chan M, Rogers Z, Bishop DT, Newton-Bishop JA. Environmental exposures such as smoking and low vitamin D are predictive of poor outcome in cutaneous melanoma rather than other deprivation measures. J Invest Dermatol 2020;140:327–37.e2.

Hogan KT, Coppola MA, Gatlin CL, Thompson LW, Shabanowitz J, Hunt DF, et al. Identification of novel and widely expressed cancer/testis gene isoforms that elicit spontaneous cytotoxic T-lymphocyte reactivity to melanoma. Cancer Res 2004;64:1157–63.

Hogan SA, Levesque MP, Cheng PF. Melanoma immunotherapy: next-generation biomarkers. Front Oncol 2018;8:178.

Jacquelot N, Belz GT. Type 2 innate lymphoid cells: a novel actor in anti-melanoma immunity. Oncoimmunology 2021;10:1943168.

Jacquelot N, Seillet C, Wang M, Pizzolla A, Liao Y, Hediyeh-Zadeh S, et al. Blockade of the co-inhibitory molecule PD-1 unleashes ILC2-dependent antitumor immunity in melanoma. Nat Immunol 2021;22:851–64.

Jewell R, Elliott F, Laye J, Nsengimana J, Davies J, Walker C, et al. The clinicopathological and gene expression patterns associated with ulceration of primary melanoma. Pigment Cell Melanoma Res 2015;28:94–104.

Joosse A, Collette S, Suciu S, Nijsten T, Patel PM, Keilholz U, et al. Sex is an independent prognostic indicator for survival and relapse/progression-free survival in metastasized stage III to IV melanoma: a pooled analysis of five European Organisation for Research and Treatment of Cancer randomized controlled trials. J Clin Oncol 2013;31:2337–46.

Krieg C, Nowicka M, Guglietta S, Schindler S, Hartmann FJ, Weber LM, et al. High-dimensional single-cell analysis predicts response to anti-PD-1 immunotherapy. Nat Med 2018;24:144–53.

Krijgsman D, de Vries NL, Skovbo A, Andersen MN, Swets M, Bastiaannet E, et al. Characterization of circulating T-, NK-, and NKT cell subsets in patients with colorectal cancer: the peripheral blood immune cell profile. Cancer Immunol Immunother 2019;68:1011–24.

Lakoski SG, Cushman M, Criqui M, Rundek T, Blumenthal RS, D'Agostino RB Jr, et al. Gender and C-reactive protein: data from the Multiethnic Study of Atherosclerosis (MESA) cohort. Am Heart J 2006;152:593–8.

Liu Y, Peng W, Li Y, Wang B, Yu J, Xu Z. Vitamin D deficiency harms patients with coronary heart disease by enhancing inflammation. Med Sci Monit 2018;24:9376–84.

Liu Y, Zugazagoitia J, Ahmed FS, Henick BS, Gettinger SN, Herbst RS, et al. Immune cell PD-L1 colocalizes with macrophages and is associated with outcome in PD-1 pathway blockade therapy. Clin Cancer Res 2020;26:970–7.

Muralidhar S, Filia A, Nsengimana J, Poźniak J, O'Shea SJ, Diaz JM, et al. Vitamin D-VDR signaling inhibits Wnt/β-catenin-mediated melanoma progression and promotes antitumor immunity. Cancer Res 2019;79:5986–98.

Naik A, Monjazeb AM, Decock J. The obesity paradox in cancer, tumor immunology, and immunotherapy: potential therapeutic implications in triple negative breast cancer. Front Immunol 2019;10:1940.

Newman AM, Gentles AJ, Liu CL, Diehn M, Alizadeh AA. Data normalization considerations for digital tumor dissection. Genome Biol 2017;18:128.

Ochoa-Hernández AB, Ramos-Solano M, Meza-Canales ID, García-Castro B, Rosales-Reynoso MA, Rosales-Aviña JA, et al. Peripheral T-lymphocytes express WNT7A and its restoration in leukemia-derived lymphoblasts inhibits cell proliferation. BMC Cancer 2012;12:60.

Park CK, Dahlke EJ, Fung K, Kitchen J, Austin PC, Rochon PA, et al. Melanoma incidence, stage, and survival after solid organ transplant: a population-based cohort study in Ontario, Canada. J Am Acad Dermatol 2020;83:754–61.

Poźniak J, Nsengimana J, Laye JP, O'Shea SJ, Diaz JMS, Droop AP, et al. Genetic and environmental determinants of immune response to cutaneous melanoma. Cancer Res 2019;79:2684–96.

Ridker PM, MacFadyen JG, Thuren T, Everett BM, Libby P, Glynn RJ, et al. Effect of interleukin-1β inhibition with canakinumab on incident lung cancer in patients with atherosclerosis: exploratory results from a randomised, double-blind, placebo-controlled trial. Lancet 2017;390:1833–42.

Shen-Orr SS, Furman D, Kidd BA, Hadad F, Lovelace P, Huang YW, et al. Defective signaling in the JAK-STAT pathway tracks with chronic inflammation and cardiovascular risk in aging humans. Cell Syst 2016;3:374–84.e4.

Storr SJ, Safuan S, Mitra A, Elliott F, Walker C, Vasko MJ, et al. Objective assessment of blood and lymphatic vessel invasion and association with macrophage infiltration in cutaneous melanoma. Mod Pathol 2012;25:493–504.

Tao Y, Shen H, Liu Y, Li G, Huang Z, Liu Y. IL-23R in laryngeal cancer: a cancer immunoediting process that facilitates tumor cell proliferation and results in cisplatin resistance. Carcinogenesis 2021;42:118–26.

Yan Z, Gibson SA, Buckley JA, Qin H, Benveniste EN. Role of the JAK/STAT signaling pathway in regulation of innate immunity in neuroinflammatory diseases. Clin Immunol 2018;189:4–13.

Yi JS, Ready N, Healy P, Dumbauld C, Osborne R, Berry M, et al. Immune activation in early-stage non-small cell lung cancer patients receiving neoadjuvant chemotherapy plus ipilimumab. Clin Cancer Res 2017;23:7474–82.

Yoshida T, Ichikawa J, Giuroiu I, Laino AS, Hao Y, Krogsgaard M, et al. C reactive protein impairs adaptive immunity in immune cells of patients with melanoma. J Immunother Cancer 2020;8:e000234.

Yuan TA, Lu Y, Edwards K, Jakowatz J, Meyskens FL, Liu-Smith F. Race-, age-, and anatomic site-specific gender differences in cutaneous melanoma suggest differential mechanisms of early- and late-onset melanoma. Int J Environ Res Public Health 2019;16:908.

Zhang Y, Wang H. Integrin signalling and function in immune cells. Immunology 2012;135:268–75.

SUPPLEMENTARY RESULTS

Questionnaire data

There was no difference in reported atopy, but women were more likely to have reported a history of autoimmune disease at age <65 years. There were no differences by sex in the highest education level achieved or in a number of factors hypothesized to be associated with inflammation, namely, recent infection of surgical wounds, sleep deprivation, and reported physical activity.

Analysis of clinical blood analyses

Supplementary Tables S3–5 show the means and SDs of the blood markers as determined by Coulter counter as well as the association between our primary measures of systemic inflammation (high-sensitivity CRP and fibrinogen) plus vitamin D levels and our poor prognosis measures (high Breslow thickness, ulceration). Supplementary Tables S3 and S4 shows the results when the blood markers are considered on a continuous scale, whereas Supplementary Table S5 shows the results when analysis involves participants outside the normal range. For the most informative statistical analysis, we focus on Supplementary Tables S3 and S4 but include Supplementary Table S5 for comparison with normal clinical measures. Supplementary Table S6 shows the distribution of prevalence of Breslow thickness, ulceration, and tumor-infiltrating lymphocytes in the population studied.

SUPPLEMENTARY MATERIALS AND METHODS

The vitamin D and immunity study

Patients presenting to the Leeds Teaching Hospitals NHS Trust melanoma multidisciplinary team (Leeds Melanoma Multidisciplinary Clinic) with newly diagnosed, primary melanoma of American Joint Committee on Cancer stage IB or higher were eligible. In the last year of recruitment, eligibility was limited to those with stage IIA or higher to enhance the proportion of the dataset with tumors of poorer prognosis. In the United Kingdom, referral to the Leeds Melanoma Multidisciplinary Clinic is mandatory, so participants were geographically ascertained.

Blood sampling

For preparation of blood for the transcriptomic analysis, 9 ml of blood in EDTA tube were passed through a LeukoLOCK filter within 2 hours of venepuncture to collect cells from which RNA was extracted.

Generation of hematological and inflammatory marker data from blood samples

Circulating white cell counts were generated by the Leeds Teaching Hospitals Trust NHS laboratory (Leeds Teaching Hospitals NHS Trust Blood Sciences) using standard Coulter counter methodology. Measuring IL-6 levels is difficult because of stability issues, so generally speaking, high-sensitivity CRP has been preferred as a measure of inflammation in similar studies, and we have measured this acute-phase protein in the study. We also measured fibrinogen levels as a second acute-phase protein, previously shown to predict cardiovascular disease (Reinhart, 2003), and because elevation of >1 acute-phase protein has been reported to further increase the risk of cardiovascular pathology (Koenig, 2003). Sera and plasma were processed on the same day by the NHS laboratories in Leeds to generate high-sensitivity CRP and fibrinogen (g/l) levels, respectively. Measurement of serum vitamin D_2/D_3 was carried out using the Siemens ADVIA Centaur XP immunoassay because ulceration was previously reported to be associated with vitamin D deficiency (Newton-Bishop et al., 2015). Measurement of aspartate transaminase, alanine transaminase (spectrophometric assay using the Siemens ADVIA chemistry 1800), and lactate dehydrogenase (ADVIA Chemistry XPT System) was carried out by Leeds Teaching Hospitals NHS Trust Clinical Biochemistry Laboratories.

Preprocessing of GeneChip Human Transcriptome Array 2.0 array data

The output CEL files were individually evaluated for pre-normalization quality control measures (eg, probe cell intensity) using Expression Console, version 1.4.1 (Affymetrix). Multiarray preprocessing at gene level was performed using the apt-probe set-summarize application of the Affymetrix Power Tools suite. This was performed on MARC1, part of the high-performance computing and Leeds Institute for Data Analytics facilities at the University of Leeds. The SST-RMA (Signal Space Transformation Robust Multichip Analysis) algorithm was used, which applies GC correction background reduction through GC count leveling and signal space transformation intensity normalization to the standard robust multichip analysis background adjustment, quantile normalization, and summarization workflow. The resulting CHP files for each sample were assessed for a number of quality control metrics to assess the success of the normalization step using Expression Console, version 1.4.1 (Affymetrix), including signal intensity, signal histogram, principal components analysis, area under the curve of positive and negative control probes, and the mean absolute deviation of the residuals from the median for all probe sets. This step identified 2 samples, which had problematic data and were excluded from all downstream analyses.

A summarized dataset containing patient metadata, summarized gene expression intensities (transcript clusters, n = 67,528), and probe set annotations for all arrays was compiled using R (version 3.5.3). Batch correction was performed using the combat package (https://www.bu.edu/jlab/wp-assets/ComBat/Abstract.html). Downstream analysis was performed either using R or Stata 14 as described. For all analyses, only those transcript clusters that were assigned a gene symbol (n = 33,494) were considered.

Identification of differentially expressed genes

Differentially expressed genes associated with each of the variables of interest were identified using limma (Linear Models for Microarray Data) Bioconductor package in R, which is designed for analyzing complex experiments with a variety of experimental conditions and predictors. Linear models were computed for each transcript cluster against each target variable adjusted for age and/or sex in the model as appropriate. Model result output includes $\log_2$(fold changes), standard errors, t-statistics, and *P*-values. The basic statistic used for significance analysis is the moderated t-statistic, which is computed for each transcript cluster and for each variable contrast. This differs from the ordinary t-statistic because the standard errors have been moderated across genes, that is, squeezed toward a common value, using a

simple Bayesian model. *P*-values arising from the moderated t-statistic have increased degrees of freedom, reflecting the greater reliability associated with smoothed standard errors. False discovery rate correction was performed using the Benjamini and Hochberg method. In cases where <1000 transcript clusters were determined to be differentially expressed with an false discovery rate <0.05, the list of genes significant with an unadjusted $P < .05$ was taken for downstream analysis to maximize input for pathway enrichment analysis.

We conducted differentially expressed genes analysis using primarily measures of gene expression obtained by averaging expression across the probes for each identified gene; the top genes identified in each analysis are given in supplementary tables. When results for an outcome show significance ($P < .05$) after adjustment for multiple testing, we also report analysis of each probe for completeness in subsequent tables.

MetaCore pathway enrichment analysis

To understand the genes that were differentially expressed in each analysis in a wider context, we used the browser-based MetaCore software package (Clarivate Analytics) to perform an enrichment analysis using a comprehensive and well-known curated database of protein–protein and protein–DNA interactions, signaling and metabolic pathways, transcription factor targets, as well as disease pathways reported in the literature. Gene identifiers of differentially expressed genes in the uploaded dataset are mapped to gene identifiers within the MetaCore database. The analysis produced outputs corresponding to various ontological entities: the highest rated (by *P*-value) pathway maps, gene ontology processes, process networks, and diseases. Additional network analysis calculations were also performed to identify the most relevant biological networks by prioritizing the number of fragments of canonical pathways in the network.

SUPPLEMENTARY REFERENCES

Koenig W. Fibrin(ogen) in cardiovascular disease: an update. Thromb Haemost 2003;89:601–19.

Newton-Bishop JA, Davies JR, Latheef F, Randerson-Moor J, Chan M, Gascoyne J, et al. 25-Hydroxyvitamin D2 /D3 levels and factors associated with systemic inflammation and melanoma survival in the Leeds Melanoma Cohort. Int J Cancer 2015;136:2890–9.

Reinhart WH. Fibrinogen–marker or mediator of vascular disease? Vasc Med 2003;8:211–6.

Gene	Fold Change	*P*-value	Adjusted *P*-value
MIR1256	1.02806	6.13E-06	0.05442
NCR3	−1.02388	1.18E-05	0.05442
NCR3	−1.02343	1.46E-05	0.05442
LOC339874	1.01873	1.70E-05	0.05682
ITPR2	1.02003	4.97E-05	0.15131
RNF4	−1.01422	6.15E-05	0.17170
IL15	1.02023	7.70E-05	0.19849
MIR1200	1.03966	9.21E-05	0.22024
LRRFIP2	1.01561	0.00010	0.22819
NF1P2	1.01106	0.00011	0.22819
IRS1	1.01102	0.00012	0.22819
KCNQ1OT1	1.01241	0.00012	0.23052
LRRC23	−1.00511	0.00014	0.24087
LINC01176	1.01519	0.00018	0.30485
CTAGE6	1.01550	0.00021	0.33118
ETFA	1.01353	0.00022	0.33118
MIR645	1.02426	0.00024	0.33394
CBLL1	−1.02553	0.00024	0.33394
LOC644919	1.02182	0.00025	0.33544
DPH2	−1.00855	0.00027	0.34647
MIR378E	1.02131	0.00034	0.37007
PGM5P2	1.01464	0.00035	0.37007
LOC440910	1.01040	0.00036	0.37007
GGT1	−1.01112	0.00040	0.37007
TMEM14EP	1.02903	0.00041	0.37007
SH3GL1P1	1.01256	0.00042	0.37007
NBPF9	1.01937	0.00044	0.37007
TXNDC16	1.01220	0.00045	0.37007
BNC2	1.01997	0.00046	0.37007
TNFRSF25	−1.00527	0.00050	0.37007
MARS2	−1.01261	0.00050	0.37007
RNU6-53P	1.01558	0.00051	0.37007
TTC22	−1.00704	0.00051	0.37007
LOC642533	1.01219	0.00053	0.37007
CLEC1A	1.01642	0.00053	0.37007

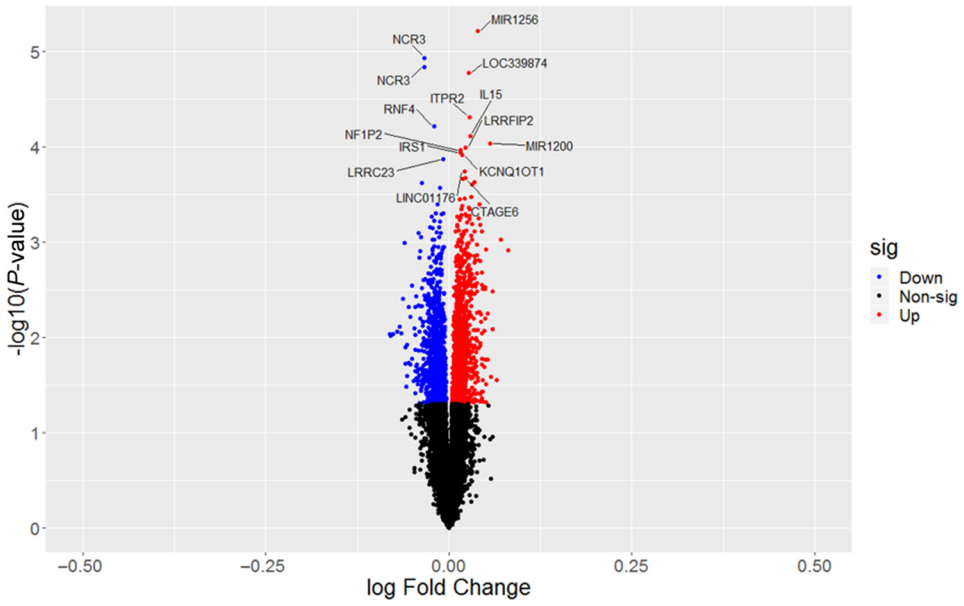

Supplementary Figure S1. The table lists the top genes differentially expressed in circulating immune cells in association with tumor thickness. The full list is provided in Supplementary Table S8. The volcano plot illustrates this, where the blue dots are genes significantly downregulated in association with tumor thickness, and red dots denote the upregulated genes.

METACORE QUICK REFERENCE GUIDE

USER DATA

NETWORKS

Up-regulated (+)
Object has user data with positive value

Down-regulated (–)
Object has user data with negative value

Mixed-signal (+/–)
Object has user data with both positive and negative values

MAPS

NETWORK OBJECTS

ENZYMES

Generic enzyme

KINASEP
- Generic kinase
- Protein kinase
- Lipid kinase

HOSPHATASE
- Generic phosphatase
- Protein phosphatase
- Lipid phosphatase

PHOSPHOLIPASE
- Generic phospholipase

PROTEASE
- Generic protease
- Metalloprotease

GTPASE
- G-alpha
- RAS - superfamily

GENERIC CLASSES

- Receptor ligand
- Transcription factor
- Protein
- Compound
- Predicted metabolite or user's structure
- Inorganic ion
- Reaction
- DNA
- RNA
- Generic binding protein

CHANNELS/TRANSPORTERS

- Generic channel
- Ligand-gated ion channel
- Voltage-gated ion channel
- Transporter

RECEPTORS

- Generic
- GPCR
- Receptors with kinase activity

G PROTEIN ADAPTOR/REGULATORS

- G beta/gamma
- Regulators (GDI, GAP, GEF, etc.)

GROUPS OF OBJECTS

A complex or a group
Proteins physically connected into a complex or related as a family

Logical association
Proteins linked by logical relations or physical interactions

Custom association
Group of collapsed objects chosen by user

INTERACTIONS BETWEEN OBJECTS

EFFECTS

- Positive / activation
- Negative / inhibition
- Unspecified

MECHANISMS

PHYSICAL INTERACTIONS

- Binding — Compound binds the enzyme or receptor
- Cleavage — Cleavage of a protein at a specific site yielding distinctive peptide fragment s. Proteolytic cleavage can be carried out by both enzymes and compound s
- Covalent modifications — Protein activity regulation by covalent binding of a small chemical group to the aminoacids of an active site.
- Phosphorylation — Protein activity is altered via addition of a phosphate group
- Dephosphorylation — Protein activity is altered via removal of a phosphate group
- Transformation — Protein activity regulation by binding & hydrolysis of GTP
- Transport — Transport of a protein or a compound between organelle s
- Catalysis — Catalysis of an enzymatic reaction
- Transcription regulation — Physical binding of a transcription factor to target gene's promot er
- MicroRNA binding — Regulation of gene expression by binding of microRNA to target mR NA

FUNCTIONAL INTERACTIONS

- Influence on expression — Compounds change the expression level of target genes indirectly , for instance by binding to upstream receptors
- Competition — Protein activity regulation by competition at the substrate binding si te
- Unspecified interactions — Mechanism is unknown or/and effect is indire ct
- Drug-Drug interactions. Pharmacological effect — Drugs change pharmacological effects of other drugs, for instance b y competing for drug metabolism enzymes or organic transporte rs
- Drug-Drug interactions. Toxic effect — Drugs change toxic effects of other drugs, for instance by competing fo r drug metabolism enzymes or organic transporters

LOGICAL RELATIONS

- Group relation — Object belongs to a generic group of related objects
- Complex subunit — Protein is a subunit of a protein complex
- Similarity relation — Chemically similar compounds with chosen Tanimoto similarity scor e

LINKS ON NETWORKS

Incoming interaction
When the mouse is over object, yellow linkindicates direction to objet

Outgoing interaction
Cyan link indicates direction FROM the object

INTERACTIONS FROM CUSTOM LIST (MetaLink™)

Interaction is in the network
Interaction is represented by a thin solid line and is highlighted in blu

Interaction is in the base, but not in network
Interaction is highlighted in yellow

Interaction is in the network
Interaction is highlighted in magenta

CANONICAL PATHWAYS

Canonical pathway
The link is highlighted in a thick cyan or magenta line

LINKS ON MAPS

- Disrupts in disease
- Weakens in disease
- Emerges in disease
- Enhances in disease
- Species specific interactions

OBJECTS ON MAPS

LOCALIZATION

- Mitochondria
- EPR
- Golgi
- Nucleus
- Lysosome
- Peroxisome
- Cytoplasm
- Extracellular

OTHER MAP OBJECTS

- Note
- Normal process
- Pathological process
- Normal map
- Disease map
- Species specific object
- Path start

THOMSON REUTERS REGIONAL OFFICES

North America
Philadelphia +1 800 336 4474
+1 215 386 0100

Latin America
+55 11 8370 9845

Europe, Middle East and Africa
Barcelona +34 93 459 2220
London +44 20 7433 4000

Asia Pacific
Singapore +65 6775 5088
Tokyo +81 3 5218 6500

Contact us to find out more about *MetaCore* or visit
thomsonreuters.com/diseaseinsight

For a complete office list visit:
science.thomsonreuters.com/contact

LS0611235

THOMSON REUTERS™

Supplementary Figure S2. The MetaCore guide to the symbols used.

a

	Maps	Total	p-value	FDR	In Data	Network Objects from Active Data
1	Cytoskeleton remodelling: Regulation of actin cytoskeleton organization by the kinase effectors of Rho GTPases	58	4.785E-16	6.021E-13	26	Vinculin, LIMK, LIMK1, MLCK, Actomyosin, Myosin II, MRLC, Paxillin, PAK, MyHC, F-Actin cytoskeleton, Actin cytoskeletal, Talin, SLC9A1, Caldesmon, ARPC1B, WRCH-1, Cdc42 subfamily, Alpha-actinin, Filamin A, RhoA-related, RhoC, Citron, PRK1, Cofilin, non-muscle, Cofilin
2	Immune response: IFN-alpha/beta signaling via JAK/STAT	64	8.553E-16	6.021E-13	27	IRF1, ISG54, ISGF3, STAT2, STAT1/STAT2, IFNAR1, IFN-alpha/beta receptor, GBP1, Apo-2L(TNFSF10), PIG3, RSAD2, PML, IRF9, OAS1, STAT5, TAP1 (PSF1), RIG-G, IL1RN, IRF7, IFI27, STAT1, IFI17, p21, ADAR1, SOCS3, STAT3, IFNAR2
3	Attenuation of IFN type I signaling in melanoma cells	37	1.226E-14	5.753E-12	20	IRF1, ISGF3, STAT2, IFNAR1, IFN-alpha/beta receptor, Apo-2L(TNFSF10), HLA-A, p38alpha (MAPK14), PSMB8(LMP7), IRF9, TAP, TAP1 (PSF1), STAT1, PSMB9, TAP2 (PSF2), Tapasin, p21, VAV-1, STAT3, IFNAR2
4	Immune response: TLR2 and TLR4 signaling pathways	69	7.500E-14	2.640E-11	26	CD36, AP-1, IL-10, NF-kB, IRAK2, p38 MAPK, TPL2(MAP3K8), MEK6(MAP2K6), TLR2, ERK1/2, I-kB, MyD88, Lyn, IRAK4, MEK3(MAP2K3), TLR1, NF-kB1 (p105), TNF-alpha, IL-1 beta, IKK-gamma, TLR6, MD-2, VAV-1, p90Rsk, Hck, TLR10
5	Immune response: IFN-gamma signaling via MAPK	51	2.348E-13	6.612E-11	22	IRF1, IFI16, p38 MAPK, IFNGR1, IFN-gamma receptor, MEK6(MAP2K6), ATF-6 alpha (50kDa), ERK1/2, IRF9, MNK1, IFNGR2, MyD88, UBCH8, MEK3(MAP2K3), TNF-alpha, STAT1, Pyk2(FAK2), C/EBPbeta, SP100, JAK2, MLK3(MAP3K11), p90RSK1

b

Pathway 2

d

Pathway 1

c

	Maps	Total	p-value	FDR	In Data	Network Objects from Active Data
1	Immune response: Induction of the antigen presentation machinery by IFN-gamma	53	4.503E-08	3.511E-05	14	JAK1, MHC class II, HLA-DQB1, HLA-DMA, HLA-DRB1, Nucleophosmin, HLA-DMB, HLA-DQA1, HLA-DRA1, HLA-DOA, HLA-DPB1, Sirtuin1, HLA-DPA1, CIITA
2	Development: WNT/Beta-catenin signaling in the nucleus	62	5.386E-08	3.511E-05	12	Frizzled, Kaiso, hSPT3, GCN5, TNIK, JNK(MAPK8-10), TBP, EP400, AF-10, BCL9/B9L, MEF2, NIPBL, Tcf(Lef), TCF7 (TCF1), RUNX
3	Immune response: Role of DAP12 receptors in NK cells	55	3.795E-06	1.643E-03	14	KIR2DL1, NKG2C, KIR2DS2, PKC-theta, KIR3DL1, Fyn, PI3K reg class IA, SOS, KIR2DL4, KIR2DL3, KIR2DL2, PLC-gamma 1
4	Development: Positive regulation of WNT/Beta-catenin signaling in the cytoplasm	76	5.039E-06	1.643E-03	11	AKT(PKB), Frizzled, HECTD1, HSP105, Axin, PKA-cat (cAMP-dependent), SIAH1, JNK(MAPK8-10), TGT, SMAD4, PPP2R2A, Tcf(Lef), Jouberin, Trabid
5	CHDI: Correlations from Replication data - Causal network (positive correlations)	79	8.075E-06	1.649E-03	11	ITK, AKT(PKB), MSK1/2 (RPS6KA5/4), MHC class II, PKC-theta, CREB1, CD3, PI3K reg class IA (p85), HSP70, JNK(MAPK8-10), MEF2, IP3 receptor, IP3R1, PLC-gamma 1

Supplementary Figure S3. MetaCore pathway analysis of genes upregulated and downregulated in the circulating immune cells of participants with increasing hsCRP. Figure was generated using the MetaCore pathway analysis tool. The genes analyzed are those significantly associated at a significance of $P < .05$, adjusted for sex and age. (**a**) The top 5 pathways identified as significantly associated with hsCRP level for upregulated genes. (**b**) The MetaCore-derived figure illustrating the differential expression of genes in the upregulated pathway map entitled immune response IFN-α/β signaling through Jak/STAT. In MetaCore images, the thermometer-like symbols adjacent to the gene name indicate genes upregulated (thermometer is red) or downregulated (thermometer is blue. (**c**) The top 5 pathways identified in association with hsCRP level for downregulated genes. (**d**) Bottom left of the figure: the MetaCore-derived image illustrating the of top scoring downregulated pathway map labeled immune response induction of the antigen-presentation machinery by IFN-γ. hsCRP, high-sensitivity CRP; STAT, signal transducer and activator of transcription.

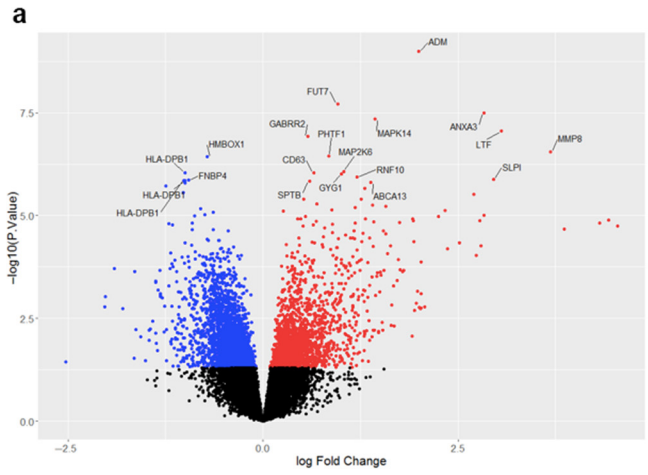

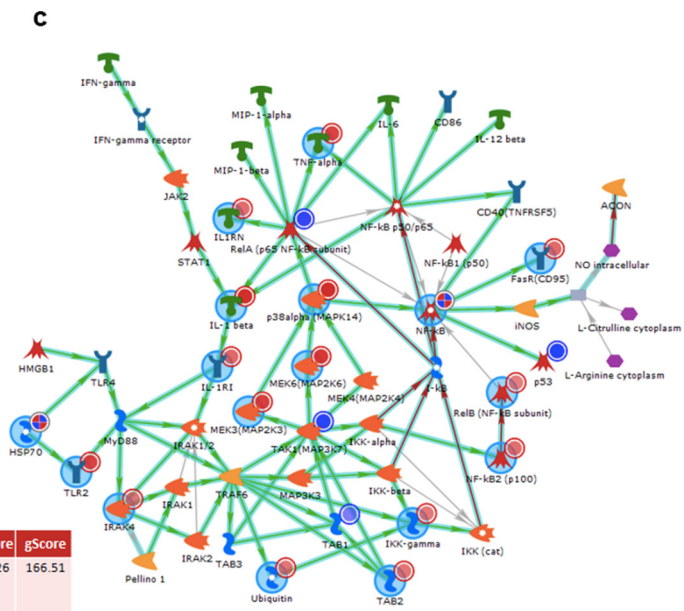

b	Network name	Processes	Size	Target	Pathways	p-Value	zScore	gScore
1	Akt(PKB), TCIRG1 (Atp6i), Galpha(i)-specific peptide GPCRs, Gastrin 17, MATK	regulation of cell population proliferation (80.4%), cellular response to oxygen-containing compound (73.9%), response to oxygen-containing compound (82.6%), regulation of smooth muscle cell proliferation (43.5%), cell surface receptor signaling pathway (84.8%)	55	7	117	3.24e-11	20.26	166.51

Supplementary Figure S4. Fibrinogen pathway analysis. (**a**) A volcano plot of the genes differentially expressed in association with serum fibrinogen level, at the significance level of $P < .05$ in an age- and sex-adjusted analysis. Blue dots represent genes expressed at a lower level in associated with higher fibrinogen levels, and red dots represent those genes differentially upregulated in participants with higher fibrinogen levels. (**b**) The network significantly associated with fibrinogen level is listed, whose process relates to proliferation pathways. (**c**) The MetaCore-derived figure representing this network identified in association with higher fibrinogen levels whose nodal genes (large sky-blue halos) include those coding for IL-1β and TLR2. Akt, protein kinase B; TLR2, toll-like receptor 2.

a

Gene	Fold Change
RNASE2	−1.05230
SLCO4C1	−1.04953
CLC	−1.04762
PI3	−1.04447
ADGRE1	−1.04359
NKG7	−1.04040
NKG7	−1.04027
FGFBP2	−1.03990
RNASE3	−1.03952
SH2D1B	−1.03801
GSTM4	−1.03671
SNORA22	−1.03599
COX8A	−1.03482
GNLY	−1.03412
CEACAM1	−1.03310
KLRF1	−1.03261
MMP9	−1.03240
PRF1	−1.03170
TARP	−1.03120
IL18RAP	−1.03092
ECRP	−1.03063
HCAR3	−1.03043
CTSW	−1.03007
LTB	−1.02981
CLIC3	−1.02970
MS4A2	−1.02925
IL2RB	−1.02778
SHKBP1	−1.02754
LPCAT2	−1.02683
GRN	−1.02653
FAM43A	−1.02645
CMKLR1	−1.02613
HCST	−1.02570
PJA2	−1.02470
COPE	−1.02468

b

	Maps	Total	*P*-value	FDR	In Data	Network Objects from Active Data
1	Protein folding and maturation: POMC processing	30	6.753E-18	8.948E-15	17	Joining peptide (JP), beta-Endorphin extracellular region, gamma-MSH, alpha-MSH, CLIP, N-POC, beta-MSH, proACTH, POMC, DA-alphaMSH, gamma2-MSH, gamma3-MSH, ACTH, N-POMC, gamma-LPH, beta-LPH, ACTH 1-17
2	Role of IL-8 in melanoma	36	1.799E-08	1.192E-05	11	AKT(PKB), VEGF-A, ITGAM, alpha-M/beta-2 integrin, IL8RB, p38 MAPK, ITGB2, G-protein alpha-i family, ERK1/2, RelA (p65 NF-kB subunit), NF-kB
3	Signal transduction: Adenosine A3 receptor signaling pathway	48	4.673E-07	2.064E-04	11	AKT(PKB), VEGF-A, Rho GTPase, p38 MAPK, Adenylate cyclase, G-protein alpha-i family, G-protein alpha-i2, ERK1/2, RelA (p65 NF-kB subunit), BAD, PLC-beta
4	Immune response: CRTH2 signaling in Th2 cells	44	1.699E-06	4.756E-04	10	AKT(PKB), ITGAM, alpha-M/beta-2 integrin, Adenylate cyclase, ITGB2, G-protein alpha-i family, CRTH2, Caspase-9, BAD, PLC-beta
5	Cell adhesion: Integrin inside-out signaling in neutrophils	77	1.795E-06	4.756E-04	13	alpha-M/beta-2 integrin, IL8RB, p38 MAPK, iNOS, FGR, DAP12, ITGB2, G-protein alpha-i family, G-protein alpha-i2, PSGL-1, L-selectin, PTAFR, PLC-beta2

c

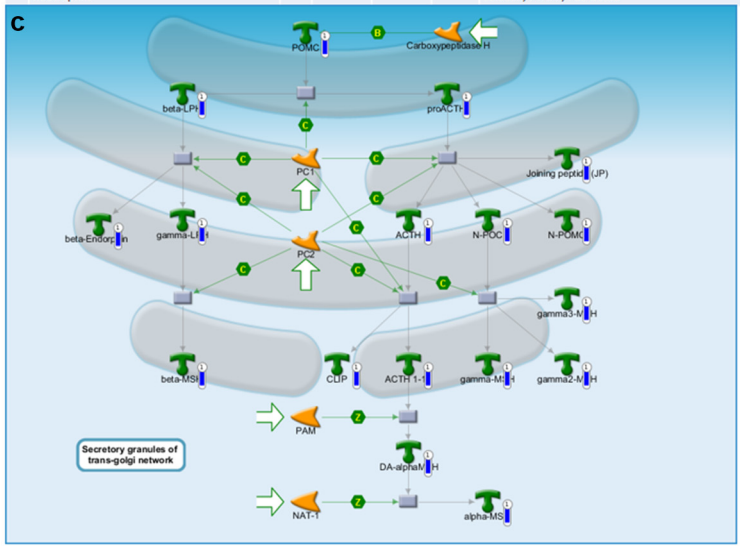

Pathway 1

Supplementary Figure S5. MetaCore pathway analysis of genes downregulated in the circulating immune cells of participants with increasing Breslow thickness adjusted for age and sex. The genes analyzed are those associated at a significance of $P < .05$ before adjustment for multiple testing. (**a**) A list of the top downregulated genes in association with thicker tumors. (**b**) The top 5 pathways identified in association with downregulated genes. (**c**) A MetaCore-derived figure illustrating the top scoring downregulated pathway in circulating immune cells of people with thicker tumors labeled protein and maturation and pro-opiomelanocortin processing.

a

	Maps	Total	p-value	FDR	In Data	Network Objects from Active Data
1	Transport: The role of AVP in regulation of Aquaporin 2 and renal water reabsorption	50	5.445E-07	5.070E-04	7	PRKAR2A, PKA-reg type II (cAMP-dependent), PKA-reg (cAMP-dependent), CREB1, MLCK, MRLC2, MRLC
2	Transcription: CREM signaling in testis	22	2.002E-06	9.320E-04	5	CREM (repressors), CREM (activators), PKA-reg (cAMP-dependent), CREB1, TSSK2
3	Immune response: Histamine signaling in dendritic cells	51	1.033E-05	3.205E-03	6	CREM (repressors), PKA-reg (cAMP-dependent), Histamine H3 receptor, CREB1, IP3 receptor, TNF-alpha
4	Muscle contraction: GPCRs in the regulation of smooth muscle tone	83	1.730E-05	4.026E-03	7	TRPC1, PKA-reg (cAMP-dependent), NCX1, Telokin, MLCK, IP3 receptor, MRLC
5	Calcium-dependent regulation of normal and asthmatic smooth muscle contraction	69	5.948E-05	9.015E-03	6	TRPC1, NCX1, MYLK1, MLCK, IP3 receptor, MRLC

b

	Maps	Total	p-value	FDR	In Data	Network Objects from Active Data
1	Maturation and migration of dendritic cells in skin sensitization	41	5.591E-07	3.685E-04	7	HLA-DRB5, HLA-DRB1, HLA-DRB, MHC class II beta chain, HLA-DRB4, I-kB, HLA-DRB3
2	Development: Notch Signaling Pathway	43	1.684E-04	5.104E-02	5	DLL4, Histone H4, MYOD, Lunatic fringe, Histone H3
3	SLE genetic marker-specific pathways in T cells	101	2.323E-04	5.104E-02	7	HLA-DRB1, HLA-DRB, MHC class II beta chain, HSD17B2, I-kB, HLA-DRB3, IFN-alpha
4	NETosis in SLE	31	5.206E-04	8.577E-02	4	Histone H4, Histone H2, Histone H3, IFN-alpha
5	Transcription: Role of heterochromatin protein 1 (HP1) family in transcriptional silencing	40	1.389E-03	1.674E-01	4	Histone H4, MYOD, SETDB1, Histone H3

d

	Network name	Processes	Size	Target	Pathways	p-Value	zScore	gScore
1	Ephrin-A, Kalirin, MIF, Prolactin, MATK	enzyme linked receptor protein signaling pathway (75.6%), transmembrane receptor protein tyrosine kinase signaling pathway (66.7%), cell surface receptor signaling pathway (93.3%), ephrin receptor signaling pathway (42.2%), positive regulation of catalytic activity (71.1%)	52	6	621	9.66e-10	18.59	794.84

E

C
Pathway 1

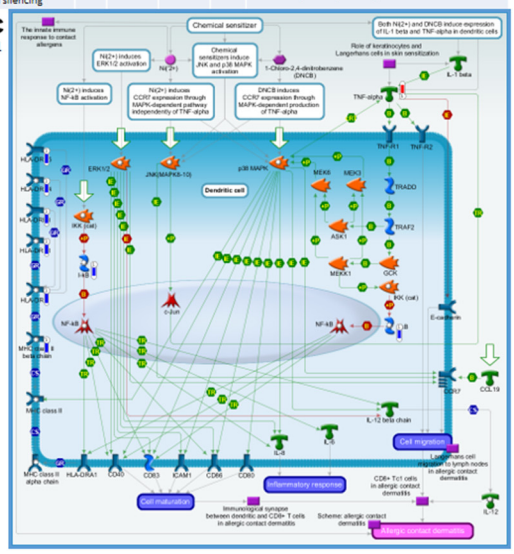

Supplementary Figure S6. MetaCore pathway analysis of genes upregulated and downregulated in the circulating immune cells of participants in association with ulceration. The genes analyzed are those associated at a significance of $P < .05$, adjusted for sex and age. (**a**) the top pathways identified for upregulated genes. (**b**) The top pathways identified for downregulated genes. (**c**) Bottom right: Details of the pathway associated with downregulated genes labeled maturation and migration of dendritic cells. (**d**) The network identified and the associated processes. (**e**) Bottom left: the process network identified for downregulated genes.

Supplementary Table S1. Description of the Reported Clinical Characteristics of the Melanoma Cases Who Participated in the Study Stratified by Age and then Sex, Followed by Information on Prevalence of Exposures Associated with Systemic Inflammation (as Taken from Literature)

	All Ages			Aged ≥65 yr			Aged >65 yr		
Trait	**Overall**	**Men**	**Women**	**Overall**	**Men**	**Women**	**Overall**	**Men**	**Women**
Clinical Characteristics									
		***t*-test: *P* = .09**			***t*-test: *P* = .03**			***t*-test: *P* = .32**	
Median age (n [range])	65.3 (391, [17 −94])	66.5 (199 [17 −88])	64.2 (192 [17 −94])	50.2 (191, [17 −64])	55.6 (92 [17 −64])	50.5 (99 [17 −64])	73.5 (200 [65 −91])	73.5 (107 [65 −88])	73.5 (93 [65 −94])
Breslow thickness, mm		**Chi-square: *P* = .03**			**Fisher: *P* = .02**			Fisher: *P* = .7	
0−1 mm	46 (11.9)	19 (9.6)	27 (14.4)	29 (15.5)	10 (11.0)	19 (19.8)	17 (8.5)	9 (8.4)	8 (8.7)
1−2 mm	101 (26.2)	42 (21.2)	59 (31.4)	57 (30.5)	22 (24.2)	35 (36.5)	44 (22.1)	20 (18.7)	24 (26.1)
2−4 mm	133 (34.5)	75 (37.9)	58 (30.9)	60 (32.1)	35 (38.5)	25 (26.0)	73 (36.7)	40 (37.4)	33 (35.9)
≥4 mm	106 (27.5)	62 (31.3)	44 (23.4)	41 (21.9)	24 (26.4)	17 (17.7)	65 (32.7)	38 (35.5)	27 (29.4)
Site of diagnosis		**Chi-square: *P* < .001**			**Fisher: *P* = .04**			**Fisher: *P* < .001**	
Trunk	138 (36.6)	88 (45.6)	50 (27.2)	78 (42.2)	43 (46.7)	35 (37.6)	60 (31.3)	45 (44.6)	15 (16.5)
Limbs	156 (41.4)	56 (29.0)	100 (54.4)	80 (43.2)	32 (34.8)	48 (51.6)	76 (39.6)	24 (23.8)	52 (57.1)
Head	56 (14.9)	39 (20.2)	17 (9.2)	16 (8.7)	12 (13.0)	4 (4.3)	40 (20.8)	27 (26.7)	13 (14.3)
Other/acral	27 (7.2)	10 (5.2)	17 (9.2)	11 (6.0)	5 (5.4)	6 (6.5)	16 (8.3)	5 (5.0)	11 (12.1)
AJCC stage at diagnosis		**Fisher: *P* = .03**			**Fisher: *P* = .02**			Fisher: *P* = .6	
I	104 (26.9)	44 (22.2)	60 (31.8)	63 (33.3)	22 (23.9)	41 (42.3)	41 (20.7)	22 (20.8)	19 (20.7)
II	185 (47.8)	100 (50.5)	85 (45.0)	78 (41.3)	42 (45.7)	36 (37.1)	107 (54.0)	58 (54.7)	49 (53.3)
III	96 (24.8)	54 (27.3)	42 (22.2)	47 (24.9)	28 (30.4)	19 (19.6)	49 (24.8)	26 (24.5)	23 (25.0)
IV	2 (0.5)	0 (0)	2 (1.1)	1 (0.5)	0 (0)	1 (1.0)	1 (0.5)	0 (0)	1 (1.1)
TILs		Chi-square: *P* = .4			Chi-square: *P* = .2			Chi-square: *P* = 1	
Not brisk	312 (84.6)	162 (86.2)	150 (82.9)	150 (83.3)	78 (86.7)	72 (80)	162 (85.7)	84 (85.7)	78 (85.7)
Brisk	57 (15.5)	26 (13.8)	31 (17.1)	30 (16.7)	12 (13.3)	18 (20)	27 (14.3)	14 (14.3)	13 (14.3)
Ulceration		Chi-square: *P* = .9			Chi-square: *P* = .7			Chi-square: *P* = .6	
No	235 (60.7)	120 (60.3)	115 (61.2)	124 (66.0)	62 (67.4)	62 (64.6)	111 (55.8)	58 (54.2)	53 (57.6)
Yes	152 (39.3)	79 (39.7)	73 (38.8)	64 (34.0)	30 (32.6)	34 (35.4)	88 (44.2)	49 (45.8)	39 (42.4)
Exposures and traits associated with current (or past) systemic inflammation									
BMI		**Fisher: *P* < .001**			**Fisher: *P* < .001**			Fisher: *P* = .2	
<18.5	2 (0.5)	0 (0)	2 (1.1)	1 (0.6)	0 (0)	1 (1.1)	1 (0.5)	0 (0)	1 (1.1)
18.5−25	106 (28.3)	37 (19.5)	69 (37.3)	63 (34.1)	18 (20.0)	45 (47.4)	43 (22.6)	19 (19)	24 (26.7)
25−30	163 (43.5)	90 (47.4)	73 (39.5)	71 (38.4)	42 (46.7)	29 (30.5)	92 (48.4)	48 (48)	44 (48.9)
≥30	104 (27.7)	63 (33.2)	41 (22.2)	50 (27.0)	30 (33.3)	20 (21.1)	54 (28.4)	33 (33)	21 (23.3)
Waist−hip ratio (WHO criteria)		**Chi-square: *P* < .001**			**Chi-square: *P* < .001**			**Fisher: *P* < .001**	
No	123 (32.9)	28 (14.7)	95 (51.9)	71 (38.8)	19 (21.1)	52 (55.9)	52 (27.2)	9 (8.9)	43 (47.8)
Yes	251 (67.1)	163 (85.3)	88 (48.1)	112 (61.2)	71 (78.9)	41 (44.1)	139 (72.8)	92 (91.1)	47 (52.2)
Highest education achieved		Chi-square: *P* = .5			Fisher: *P* = .3			Fisher: *P* = .7	
Primary/secondary	97 (33.9)	45 (30.6)	52 (37.4)	40 (29.4)	14 (21.5)	26 (36.6)	57 (38.0)	31 (37.8)	26 (38.2)
Sixth form/university (not graduated)	32 (11.2)	15 (10.2)	17 (12.2)	15 (11.0)	8 (12.3)	7 (9.9)	17 (11.3)	7 (8.5)	10 (14.7)
University (graduated)	64 (22.4)	35 (23.8)	29 (20.9)	31 (22.8)	16 (24.6)	15 (21.1)	33 (22.0)	19 (23.2)	14 (20.6)
Vocational	93 (32.5)	52 (35.4)	41 (29.5)	50 (36.8)	27 (41.5)	23 (32.4)	43 (28.7)	25 (30.5)	18 (26.5)

(*continued*)

Supplementary Table S1. Continued

Trait	All Ages			Aged ≥65 yr			Aged >65 yr		
	Overall	Men	Women	Overall	Men	Women	Overall	Men	Women
Recent infected surgical wounds		Fisher: $P = .8$			Fisher: $P = .4$			Fisher: $P = 1$	
No	345 (97.2)	172 (96.6)	173 (97.7)	170 (96.6)	81 (95.3)	89 (97.8)	175 (97.8)	91 (97.9)	84 (97.7)
Yes	10 (2.8)	6 (3.4)	4 (2.3)	6 (3.4)	4 (4.7)	2 (2.2)	4 (2.2)	2 (2.2)	2 (2.3)
History of type 2 diabetes		Fisher: $P = .2$			Fisher: $P = 1$			Fisher: $P = .2$	
No	261 (93.6)	131 (91.6)	130 (95.6)	131 (97.8)	63 (98.4)	68 (97.1)	130 (89.7)	68 (86.1)	62 (93.9)
Yes	18 (6.5)	12 (8.4)	6 (4.4)	3 (2.2)	1 (1.6)	2 (2.9)	15 (10.3)	11 (13.9)	4 (6.1)
Hypertension		**Chi-square: $P = .01$**			**Fisher: $P = .01$**			Chi-square: $P = .4$	
No	187 (67.0)	86 (60.1)	101 (74.3)	105 (78.4)	44 (68.8)	61 (87.1)	82 (56.6)	42 (53.2)	40 (60.6)
Yes	92 (32.3)	57 (39.9)	35 (25.7)	29 (21.6)	20 (31.3)	9 (12.9)	63 (43.5)	37 (46.8)	26 (39.4)
Angina/heart attack		**Fisher: $P < .001$**			Fisher: $P = .2$			**Fisher: $P = .002$**	
No	246 (88.2)	116 (81.1)	130 (95.6)	126 (94.0)	58 (90.6)	68 (97.1)	120 (82.8)	58 (73.4)	62 (93.9)
Yes	33 (11.8)	27 (18.9)	6 (4.4)	8 (6.0)	6 (9.4)	2 (2.9)	25 (17.2)	21 (26.6)	4 (6.1)
Atopy		Chi-square: $P = .09$			Chi-square: $P = .08$			Chi-square: $P = .6$	
No	223 (79.9)	120 (83.9)	103 (75.7)	102 (76.1)	53 (82.8)	49 (70)	121 (83.5)	67 (84.8)	54 (81.8)
Yes	56 (20.1)	23 (16.1)	33 (24.3)	32 (23.9)	11 (17.2)	21 (30)	24 (16.6)	12 (15.2)	12 (18.2)
History of autoimmune disease		Chi-square: $P = .07$			**Fisher: $P = .05$**			Chi-square: $P = .3$	
No	233 (83.5)	125 (87.4)	108 (79.4)	120 (89.6)	61 (95.3)	59 (84.3)	113 (77.9)	64 (81.0)	49 (74.2)
Yes	46 (16.5)	18 (12.6)	28 (20.6)	14 (10.5)	3 (4.7)	11 (15.7)	32 (22.1)	15 (19.0)	17 (25.8)
Sleep, hr		Chi-square: $P = .2$			Fisher: $P = .6$			Fisher: $P = .06$	
<7	74 (26.2)	35 (24.0)	39 (28.5)	95 (69.9)	44 (66.7)	51 (72.9)	36 (24.5)	15 (18.8)	21 (31.3)
7–9	203 (71.7)	106 (72.6)	97 (70.8)	38 (27.9)	20 (30.3)	18 (25.7)	108 (73.5)	62 (77.5)	46 (68.7)
>9	6 (2.1)	5 (3.42)	1 (0.73)	3 (2.2)	2 (3.0)	1 (1.4)	3 (2.0)	3 (3.8)	0 (0)
Activity		Chi-square: $P = .2$			Fisher: $P = 1$			Chi-square: $P = .06$	
Inactive	168 (58.1)	79 (53.0)	89 (63.6)	85 (62.0)	41 (62.1)	44 (62.0)	83 (54.6)	38 (45.8)	45 (65.2)
Minimally active	74 (25.6)	42 (28.2)	32 (22.9)	34 (24.8)	16 (24.2)	18 (25.4)	40 (26.3)	26 (31.3)	14 (20.3)
HEPA active	47 (16.3)	28 (18.8)	19 (13.6)	18 (13.1)	9 (13.6)	9 (12.7)	29 (19.1)	19 (22.9)	10 (14.5)
Smoking		**Chi-square: $P = .02$**			Fisher: $P = .8$			**Fisher: $P = .005$**	
Never	154 (53.5)	70 (47.3)	84 (60)	79 (57.7)	38 (57.6)	41 (57.8)	75 (49.7)	32 (39.0)	43 (62.3)
Previous	108 (37.5)	67 (45.3)	41 (29.3)	41 (29.9)	21 (31.8)	20 (28.2)	67 (44.4)	46 (56.1)	21 (30.4)
Current	26 (9.0)	11 (7.4)	15 (10.7)	17 (12.4)	7 (10.6)	10 (14.1)	9 (6.0)	4 (4.9)	5 (7.3)
Pack yrs, median (IQR)	15.7 (27.6)	21 (30.5)	12.4 (21.8)	20.3 (26)	29.3 (28)	15 (24.3)	10 (28.5)	10 (31.7)	9 (21.1)
Alcohol in preceding wk		**Chi-square: $P = .002$**			**Chi-square: $P = .006$**			Chi-square: $P = .06$	
No	118 (32.9)	46 (25.3)	72 (40.7)	48 (27.3)	15 (17.7)	33 (36.3)	70 (38.3)	31 (32.0)	39 (45.4)
Yes	241 (67.1)	136 (74.7)	105 (59.3)	128 (72.7)	70 (82.4)	58 (63.7)	113 (61.8)	66 (68.0)	47 (54.7)
Alcohol units preceding wk, median (IQR)	10.5 (17)	14 (20.5)	9 (12.5)	12 (16)	16 (27)	9.3 (12)	10.5 (16)	11.8 (17)	7.5 (13.5)
Aspirin (ever)		**Fisher: $P < .001$**			**Fisher: $P = .003$**			**Fisher: $P = .001$**	
No	251 (86.3)	117 (77.5)	134 (95.7)	131 (94.2)	60 (88.2)	71 (100)	120 (79.0)	57 (68.7)	63 (91.3)
Yes	40 (13.8)	34 (22.5)	6 (4.3)	8 (5.8)	8 (11.8)	0 (0)	32 (21.1)	26 (31.3)	6 (8.7)

(*continued*)

Supplementary Table S1. Continued

	All Ages			Aged ≥65 yr			Aged >65 yr		
Trait	**Overall**	**Men**	**Women**	**Overall**	**Men**	**Women**	**Overall**	**Men**	**Women**
Statins (ever)		**Chi-square: $P < .001$**			**Fisher: $P = .003$**			**Chi-square: $P = .001$**	
No	205 (70.5)	89 (58.9)	116 (82.9)	119 (85.6)	52 (76.5)	67 (94.4)	86 (56.6)	37 (44.6)	49 (71.0)
Yes	86 (29.6)	62 (41.1)	24 (17.1)	20 (14.4)	16 (23.5)	4 (5.6)	66 (43.4)	46 (55.4)	20 (29.0)
Aspirin (exposure at diagnosis)		Fisher: $P < .001$			**Fisher: $P = .01$**			**Fisher: $P = .001$**	
No	259 (89.0)	123 (81.5)	136 (97.1)	133 (95.7)	62 (91.2)	71 (100)	126 (82.9)	61 (73.5)	65 (94.2)
Yes	32 (11.0)	28 (18.5)	4 (2.9)	6 (4.3)	6 (8.8)	0 (0)	26 (17.1)	22 (26.5)	4 (5.8)
Statins (exposure at diagnosis)		**Fisher: $P < .001$**			**Fisher: $P = .006$**			**Fisher: $P = .002$**	
No	207 (71.1)	91 (60.3)	116 (82.9)	120 (86.3)	53 (77.9)	67 (94.4)	87 (57.2)	38 (45.8)	49 (71.0)
Yes	84 (28.9)	60 (39.7)	24 (17.1)	19 (13.7)	15 (22.1)	4 (5.6)	65 (42.8)	45 (54.2)	20 (29.0)

Abbreviation: AJCC, American Joint Committee on Cancer; BMI, body mass index; HEPA, health advancing physical activity score; IQR, interquartile range; TIL, tumor-infiltrating lymphocyte; WHO, World Health Organization.

Entries in each cell are numbers (and row percentage). Each statistical comparison shows the type of test (chi-square test with appropriate degrees of freedom; Fisher = Fisher exact test). Test *P*-value measures the deviation from null hypothesis of no effect. Note, there are some missing data so totals are not always exactly the same for each factor tested. Significance at the <.05 level is indicated in bold.

Supplementary Table S2. Associations between Inflammatory Markers and Clinicopathological Variables

	Fibrinogen					hsCRP				
Clinical Characteristic	**n**	**Univariable Estimate**	***P*-Value**	**Multivariable Estimate**	***P*-Value**	**n**	**Univariable Estimate**	***P*-Value**	**Multivariable Estimate**	***P*-Value**
Age (per year)	364	0.002 (0.001−0.03)	**<0.001**	0.002 (0.0006−0.0024)	**.001**	373	0.006 (0.002−0.009)	.001	0.009 (0.005−0.014)	**<.001**
Sex										
Female (baseline)	174	0	—	0	—	180	0	—		
Male	190	−0.017 (−0.037 to 0.003)	0.1	−0.028 (−0.054 to −0.002)	.04	193	−0.097 (−0.197 to 0.004)	.06	−0.158 (−0.287 to −0.028)	**.02**
Breslow thickness (mm)										
0−1	42	0.004 (−0.031 to 0.039)	0.8	−0.001 (−0.040 to 0.039)	1	44	−0.120 (−0.295 to 0.055)	.2		
1−2 (baseline)	94	0	—	0	—	98	0	—		
2−4	127	0.019 (−0.007 to 0.045)	0.2	0.021 (−0.009 to 0.052)	.1	129	−0.103 (−0.233 to 0.027)	.1		
≥4	99	0.038 (0.011−0.066)	**0.006**	0.037 (0.005−0.069)	**.02**	100	0.044 (−0.095 to 0.184)	.5		
Site of diagnosis										
Trunk (baseline)	131	0	—	0	—	135	0	—	0	—
Limbs	149	−0.001 (−0.025 to 0.023)	0.9			151	−0.018 (−0.135 to 0.099)	.8	0.008 (−0.122 to 0.138)	.9
Head	55	0.015 (−0.016 to 0.046)	0.4			54	0.120 (−0.038 to 0.278)	.1	0.170 (−0.018 to 0.342)	.05
Other/acral	25	0.006 (−0.036 to 0.048)	0.8			25	−0.085 (−0.297 to 0.126)	.4	−0.027 (−0.213 to 0.268)	.8
Stage at diagnosis										
I (baseline)	97	0	—	0	—	101	0	—	0	—
II	172	0.026 (0.002−0.051)	**0.04**			177	−0.001 (−0.124 to 0.123)	1		
III	92	0.00003 (−0.027 to 0.028)	1			92	−0.015 (−0.156 to 0.126)	.8		
IV	2	0.037 (−0.098 to 0.171)	0.6			2	0.111 (−0.683 to 0.706)	1		
TILS										
Not brisk TILs (baseline)	299	0	—	0	—	304	0	—	—	—
Brisk TILs	53	−0.005 (−0.033 to 0.024)	0.8	—	—	53	0.056 (−0.089 to 0.200)	.4	—	—
Exposures and traits associated with current (or past) systemic inflammation										
BMI										
18.5−25 (baseline)	101	0	—	0	—	103	0	—	0	—
25−30	154	0.015 (−0.009 to 0.040)	0.2	0.002 (−0.027 to 0.030)	.9	157	0.202 (0.082−0.321)	**.001**	0.200 (0.065−0.336)	**.004**
≥30	95	0.055 (0.028−0.082)	**<0.001**	0.048 (0.013−0.083)	**.03**	99	0.406 (0.273−0.539)	<.001	0.435 (0.267−0.604)	**<.001**
Waist hip ratio (WHO criteria)										
Not obese	117	0	—	0	—	117	0	—	0	—
Obese	234	0.028 (0.004−0.051)	**0.02**	0.021 (−0.008 to 0.051)	.2	243	0.162 (0.042−0.282)	**.008**	0.036 (−0.106 to 0.178)	.6
Type 2 Diabetes										
No (baseline)	247	0	—	—	—	255	0	—	0	—
Yes	18	0.027 (−0.020 to 0.075)	0.3	—	—	18	0.144 (−0.100 to 0.387)	.2	—	—
Hypertension										
No (baseline)	175	0	—			183	0	—	—	—
Yes	90	0.029 (0.003−0.055)	**0.03**	0.019 (−0.007 to 0.045)	.2	90	0.018 (−0.115 to 0.150)	.8	—	—
Angina										
No (baseline)	234	0	—	—	—	241	0	—	—	—
Yes	31	−0.006 (−0.045 to 0.032)	0.7	—	—	32	−0.134 (−0.325 to 0.057)	.2	—	—

(*continued*)

Supplementary Table S2. Continued

		Fibrinogen					hsCRP			
Clinical Characteristic	**n**	**Univariable Estimate**	***P*-Value**	**Multivariable Estimate**	***P*-Value**	**n**	**Univariable Estimate**	***P*-Value**	**Multivariable Estimate**	***P*-Value**
Atopy										
No (baseline)	213	0	—	—	—	217	0	—	—	—
Yes	52	−0.005 (−0.035 to 0.025)	0.8	—	—	56	−0.082 (−0.230 to 0.065)	.3	—	—
History of autoimmune disease										
No (baseline)	224	0	—	—	—	227	0	—	—	—
Yes	41	−0.113 (−0.044 to 0.022)	0.5	—	—	46	−0.027 (−0.188 to 0.134)	.7	—	—
Sleep										
7−9 hr (baseline)	196	0	—	—	—	199	0	—	0	—
< 7 hrs	67	0.020 (−0.007 to 0.046)	0.2	—	—	72	0.187 (0.054−0.320)	**.006**	0.122 (−0.007 to 0.252)	.06
>9 hrs	6	0.047 (−0.032 to 0.126)	0.2	—	—	6	0.372 (−0.029 to 0.773)	.07	0.234 (−0.139 to 0.608)	.2
Exercise										
Inactive (baseline)	159	0	—	0	—	165	0	—	0	—
Minimally active	71	−0.016 (−0.044 to 0.011)	0.3	−0.013 (−**0**.041 to 0.015)	.4	72	−0.223 (−0.360 to −0.087)	**.001**	−0.202 (−0.335 to −0.069)	**.003**
HEPA active	45	−0.031 (−0.063 to 0.002)	0.07	−0.018 (−0.052 to 0.016)	.3	46	−0.157 (−0.318 to 0.004)	.06	−0.087 (−0.247 to 0.073)	.3
Smoking										
Never	147	0	—	0	—	151	0	—	0	—
Previous	102	0.0003 (−0.024 to 0.026)	1	−0.003 (−0.030 to 0.023)	.8	105	−0.085 (−0.211 to 0.040)	.2	−0.027 (−0.151 to 0.097)	.7
Current	25	0.042 (0.0008−0.084)	0.05	0.017 (−0.028 to 0.062)	.5	26	0.245 (0.038−0.452)	.02	0.162 (−0.042 to 0.367)	.1
Exposure to statins										
No (baseline)	194	0	—	—	—	201	0	—	0	—
Yes	83	0.013 (−0.014 to 0.041)	0.3	—	—	84	−0.143 (−0.281 to −0.006)	.04	−0.180 (−0.327 to −0.032)	**.02**
Statin exposure at diagnosis										
No (baseline)	196	0	—	0	—	203	0	—	—	—
Yes	81	0.015 (−0.013 to 0.042)	0.3	—	—	82	−0.154 (−0.292 to −0.016)	**.03**	—	—
Exposure to aspirin										
No (baseline)	238	0	—	—	—	248	0	—	0	—
Yes	39	0.044 (−0.031 to 0.039)	0.8	—	—	37	−0.172 (−0.353 to 0.008)	.06	−0.167 (−0.366 to 0.031)	.1
Aspirin exposure at diagnosis										
No (baseline)	246	0	—	—	—	254	0	—	0	—
Yes	31	0.010 (−0.029 to 0.048)	0.6	—	—	31	−0.107 (−0.301 to 0.087)	.3	—	—

Abbreviations: HEPA, health enhancing physical activity; hsCRP, high-sensitivity CRP; TIL, tumor-infiltrating lymphocyte; WHO, World Health Organization

Analyses are performed as linear regression of log10 (fibrinogen or hsCRP) as the outcome with baseline as indicated by characteristic; the value of the regression coefficient (estimate) as well as 95% confidence interval for that estimate and *P*-value for each exposure testing evidence for nonzero effect. Table also shows multivariate analyses using those factors with $P < .1$ in univariable analyses. Significance levels at $P < .05$ are shown in bold.

Supplementary Table S3. The Association between Measured Blood Parameters and Characteristics of the Primary Tumor of Participants in Univariable Analyses

Parameter	Mean (SD)	Standard Range	Cases below Normal Range	Cases in Normal Range	Cases Elevated	Log_{10}(Breslow Thickness)		Ulceration (Yes/No)		Brisk TILs (Yes/No)	
						Estimate (SE)	*P*-Value	OR	*P*-Value	OR	*P*-Value
hsCRP	2.95 (5.48)	<6 mg/l	—	330	44	0.060 (0.073)	.4	1.15(0.75−1.77)	.5	1.25 (0.69−2.26)	.5
Fibrinogen	2.86 (0.67)	1.5−3.9 g/l	3	322	40	0.859 (0.373)	**.02**	6.11(0.65−57.8)	.1	0.60 (0.03−13.1)	.7
Vitamin D[1]	42.5 (23.2)	20−100 nmol/l	43	243	4	−0.390 (0.197)	.05	0.66 (0.20−2.17)	.5	0.71 (0.14−3.55)	.7
ALT	24.5 (16.1)	<40 iu/l	—	207	23	0.095 (0.219)	.7	0.51 (0.14−1.90)	.3	0.37 (0.06−2.34)	.3
AST	24.9 (9.55)	<40 iu/l	—	171	10	−0.387 (0.404)	.3	0.15 (0.01−2.67)	.2	6.62 (0.27−59.8)	.2
Eosinophils	0.15 (0.12)	$<0.5 \times 10^9$/l	—	280	5	−0.274 (0.127)	**.03**	0.60 (0.28−1.28)	.2	0.36 (0.12−1.04)	.06
LDH	389 (90.7)	160−430 IU/l	1	284	87	0.040 (0.049)	.4	1.33 (0.99−1.79)	.06	0.97 (0.64−1.48)	.9
Lymphocytes	1.82 (0.67)	$1.0−4.5 \times 10^9$/l	20	266	—	−0.046 (0.062)	.5	1.00 (0.69−1.43)	1	1.19 (0.73−1.96)	.5
MCH	30.2 (1.78)	25−35 pg/cell	3	282	1	−0.035 (0.023)	.1	0.93 (0.82−1.07)	.3	1.01 (0.83−1.21)	.9
MCV	92.1 (4.94)	78−100 fl	1	271	14	−0.015 (0.008)	.06	0.98 (0.94−1.03)	.5	1.05 (0.98−1.12)	.1
Monocytes	0.43 (0.18)	$0.1−0.8 \times 10^9$/l	2	279	5	−0.301(0.297)	.3	1.22 (0.21−7.15)	.8	0.44 (0.04−5.43)	.5
Neutrophils	4.77 (1.44)	$2−7.5 \times 10^9$/l	4	268	14	0.018 (0.027)	.5	1.08 (0.91−1.27)	.4	0.96 (0.76−1.22)	.8
Platelet	248.6 (62.6)	$150−400 \times 10^9$/l	12	268	6	−0.389 (0.392)	.3	0.47 (0.05−4.94)	.5	1.79 (0.06−49.6)	.7
Total WCC	10.8 (58.0)	$4−11 \times 10^9$/l	3	268	15	−0.0004 (0.022)	1	1.05 (0.92−1.20)	.5	0.99 (0.82−1.19)	.9
Neutrophil/ lymphocyte ratio (log10)			—	—	—	0.227 (0.237)	.3	1.58(0.39−6.47)	.5	0.48 (0.07−3.46)	.5

Abbreviations: ALT, alanine aminotransferase; AST, aspartate aminotransferase; hsCRP, high-sensitivity CRP; LDH, lactate dehydrogenase; MCP, mean corpuscular volume; MCV, mean corpuscular volume; SE, standard error; TIL, tumor-infiltrating lymphocyte; WCC, white cell count.

This table shows the age- and sex-adjusted univariable analysis of the associations between blood parameters at diagnosis of primary melanoma and key clinical indicators of melanoma-specific survival. Each parameter is analysed as a continuous variable.

[1]Analyses adjusted for season, assuming blood was drawn in period January−March.

Supplementary Table S4. The Association between Measured Blood Parameters and Characteristics of the Primary Tumor of Participants in Multivariable Analyses

Measured Blood Parameter	Measure of Association With Tumor Characteristics	*P*-Value
Multivariable association with Breslow thickness (adjusted for age, sex, and season of blood draw)		
	Estimate (SE)	*P*-value
Eosinophils (log_{10})	−0.340 (0.133)	.01
Fibrinogen (log_{10})	1.680 (0.429)	<.001
MCH	0.037 (0.046)	.4
MCV	−0.023 (0.017)	.2
Vitamin D (log_{10})	−0.046 (0.205)	.03
Multivariable association with ulceration (adjusted for sex)		
	OR (95% CI)	*P*-value
Eosinophils (log 10)	0.47 (0.22−1.05)	0.07
Fibrinogen (log 10)	5.88 (0.40−86.6)	0.2
LDH	1.30 (0.89−1.91)	0.2
Multivariable association with brisk TILs (adjusted for age and sex)		
	OR (95% CI)	*P*-value
Eosinophils	0.37 (0.13−1.08)	0.07
MCV	1.06 (0.99−1.14)	0.1

Abbreviations: CI, confidence interval; LDH, lactate dehydrogenase; MCP, mean corpuscular volume; MCV, mean corpuscular volume; SE, standard error; TIL, tumor-infiltrating lymphocyte.

This table shows the age- and sex-adjusted multivariable analysis of the associations between blood parameters at diagnosis of primary melanoma and key clinical indicators of melanoma-specific survival. Each parameter is analysed as a continuous variable.

Supplementary Table S5. Association of Blood Test Results with Melanoma Characteristics Presented as Results of the Normal Range Rather than as Continuous Variables (Normally Used in Clinical Work)

Parameter	Mean (SD)	Standard Range	Cases below Normal Range	Cases in Normal Range	Cases Elevated	Log_{10}(Breslow Thickness)		Ulceration		Brisk TILs (Yes/No)	
						Estimate (SE)	*P*-Value	OR	*P*-Value	OR	*P*-Value
								Elevated versus normal range			
ALT	24.5 (16.1)	<40 iu/l	—	207	23	0.062 (0.155)	.7	0.81 (0.32–2.02)	.6	0.97 (0.25–3.74)	1
AST	24.9 (9.55)	<40 iu/l	—	171	10	−0.342 (0.224)	.1	0.29 (0.04–2.39)	.3	3.58 (0.82–15.69)	.09
Eosinophils	0.15 (0.12)	$<0.5 \times 10^9$/l	—	280	5	−0.566 (0.301)	.06	0.35 (0.04–3.16)	.3	—	—
Fibrinogen	2.86 (0.67)	1.5-3.6 g/l	3	322	40	**0.230 (0.116)**	**.05**	1.89 (0.96–3.72)	.07	1.72 (0.72–4.09)	.2
HsCRP	2.95 (5.48)	<6 mg/l	—	330	44	0.047 (0.110)	.7	0.77 (0.40–1.50)	.4	1.17 (0.49–2.80)	.7
LDH	389 (90.7)	160-430 IU/l	1	284	87	0.078 (0.086)	.4	1.29 (0.79–2.12)	.3	0.75 (0.34–1.63)	.5
MCH	30.2 (1.78)	25–35 pg/cell	3	282	1	0.514 (0.672)	.4	—	—	—	—
MCV	92.1 (4.94)	78–100 fl	1	271	14	−0.165 (0.186)	.4	0.68 (0.22–2.13)	.5	3.96 (1.21–12.99)	**.02**
Monocytes	0.43 (0.18)	$0.1–0.8 \times 10^9$/l	2	279	5	−0.043 (0.303)	.9	1.95 (0.32–11.9)	.5	—	—
Neutrophils	4.77 (1.44)	$2–7.5 \times 10^9$/l	4	268	14	0.147 (0.184)	.4	1.47 (0.50–4.36)	.5	0.41 (0.05–3.23)	.4
Platelet	248.6 (62.6)	$150–400 \times 10^9$/l	12	268	6	−0.086 (0.281)	.8	1.29 (0.25–6.59)	.8	1.34 (0.15–12.04)	.8
Total WCC	10.8 (58.0)	$4–11 \times 10^9$/l	3	268	15	0.043 (0.178)	.8	1.71 (0.59–4.90)	.3	0.39 (0.05–3.08)	.4
								Below normal versus normal range			
Lymphocytes	1.82 (0.67)	$1.0–4.5 \times 10^9$/l	20	266	—	0.057 (0.157)	.7	1.01 (0.40–2.55)	1	0.73 (0.16–3.32)	.7
Platelet	248.6 (62.6)	$150–400 \times 10^9$/l	12	268	6	0.107 (0.203)	.6	1.22 (0.37–4.01)	.7	0.58 (0.07–4.82)	.6
Vitamin D[1]	42.5 (23.2)	20–100 nmol/l	43	243	4	0.235 (0.112)	**.04**	2.25 (1.16–4.38)	**.02**	0.92 (0.36–2.36)	.9

Abbreviations: ALT, alanine aminotransferase; AST, aspartate aminotransferase; hsCRP, high-sensitivity CRP; LDH, lactate dehydrogenase; MCV, mean corpuscular volume; SE, standard error; TIL, tumor-infiltrating lymphocyte; WCC, white cell count. Significance values at $P < .05$ are shown as bold.

[1]Vitamin D analysis adjusted for season, assuming blood drawn in winter.

Supplementary Table S6. Distribution of Poor Prognosis Markers among Participants in the Study

Breslow Thickness >4 mm	Ulceration	Absence of Brisk TILs	Number of Participants
Y	Y	Y	61 (17%)
Y	Y	N	5 (1%)
Y	N	Y	32 (9%)
Y	N	N	2 (1%)
N	Y	Y	66 (18%)
N	Y	N	11 (3%)
N	N	Y	152 (41%)
N	N	N	39 (11%)
Total			368 (100%)

Abbreviations: hsCRP, high-sensitivity CRP; N, no; TIL, tumor-infiltrating lymphocyte; Y, yes.

This tables shows an analysis of the distribution of the poor prognosis markers in the 355 participants in whom hsCRP level was available.